Geological Quarterly, 2024, 68, 34
DOI: http://dx.doi.org/10.7306/gq.1762

Chemical weathering indices in contrasting fluvial systems: a comparative study from the Lublin Upland and the Sudetes Mountains in Poland

Weronika NADŁONEK[1, *], Sylwia SKRECZKO[2] and Beata NAGLIK[1]

[1] Polish Geological Institute – National Research Institute, Królowej Jadwigi 1, 41-200 Sosnowiec, Poland; ORCID: 0000-0002-2675-2601 [W.N.], 0000-0002-4452-3378 [B.N.]

[2] University of Silesia in Katowice, Faculty of Natural Sciences, Będzińska 60, 41-200 Sosnowiec, Poland; ORCID: 0000-0003-2088-9313

Nadłonek, W., Skreczko, S., Naglik, B., 2024. Chemical weathering indices in contrasting fluvial systems: a comparative study from the Lublin Upland and the Sudetes Mountains in Poland. Geological Quarterly, 68, 34; https://doi.org/10.7306/gq.1762

The chemical weathering indices in different fluvial systems in Poland are determined, to indicate which factors affect small-scale chemical weathering processes to the greatest degree. The Weathering Index of Parker (WIP), Vogt's Residual Index (V), the Chemical Index of Alteration (CIA), Harnois's Chemical Index of Weathering (CIW), and the Plagioclase Index of Alteration (PIA), as well as Rb/Sr and Sr/Cu ratios, were calculated for 30 sediment samples taken from four selected rivers in the Lublin Upland and the Sudetes Mountains, respectively. The median values for the Lublin Upland rivers were as follows: WIP (12.14–13.05), V (0.66–0.83), CIA (31.79–33.93), CIW (36.67–38.07); PIA (25.20–29.84), Rb/Sr (0.32–0.41), Sr/Cu (14.01–19.66). The median values obtained in the Sudetes Mountains were: WIP (49.88–56.25), V (2.03–2.70), CIA (54.73–56.63), CIW (68.60–70.59), PIA (58.48–59.59), Rb/Sr (1.13–2.70), Sr/Cu (5.94–8.14). River sediment samples were also analysed using a scanning electron microscope and XRD diffraction of whole rock samples to identify minerals hosting the elements investigated. The results indicate a higher intensity of weathering processes in the Sudetes Mountains than in the Lublin Upland and corroborated that, besides the climate regime, other factors, such as bedrock lithology, physical erosion and landform type have significant meaning in assessing weathering processes (Graphical abstract).

Key words: modern river sediments, chemical weathering indices, factors controlling weathering intensity, fluvial systems of the Sudetes Mountains and Lublin Upland, geochemical proxies for tracking climate changes.

INTRODUCTION

Weathering of the continental crust is a crucial surficial geological process that impacts the biogeochemical cycle of carbon, ultimately regulating the Earth's climate. This is because the chemical weathering of Ca-silicates produces cations and HCO_3 which are transported to the oceans by rivers and are then consumed by carbonate precipitation onto the seafloor (e.g., Dupré et al., 2003). Rivers constitute the primary connection between land and the global ocean, and the study of weathered terrigenous materials transported by river systems provides first-hand information on various natural processes as well as on human activity within drainage basins (e.g., Guo et al., 2018). Significant research effort has been applied to understanding chemical weathering processes and quantifying the intensity of rock weathering and associated CO_2 consumption rates. Since the pioneering work of Vogt (1927), several geochemical proxies have been established to evaluate weathering regimes and reconstruct palaeoclimatic changes in catchments. Silicate weathering indices are commonly used to identify palaeoweathering processes and palaeoclimate (Yang et al., 2016; Perri, 2018; Maslov and Podkovyrov, 2023), evaluate soil fertility and development (Price and Velbel, 2003; Li and Yang, 2010; Shao et al., 2012; Chetelat et al., 2013), estimate the impact of climate on bedrock weathering (Neall, 1977), quantify the chemical alteration of source rocks, and better understand the mobility of elements during weathering processes (Fedo et al., 1995; Sharma and Rajamani, 2000). Estimating the chemical weathering indices contributes to the reconstruction of the palaeoenvironmental conditions and reflects climate changes, involved also with changes in the physical weathering processes affecting the mineralogical composition of soils and sediments. The most commonly used proxies are the Weathering Index of Parker (WIP) and the Chemical Index of Alteration (CIA; Parker, 1970; Nesbitt and Young, 1982); along with the Chemical Index of Weathering (CIW; Harnois, 1988), Vogt's Residual Index (V; Vogt, 1927), and the Plagioclase Index of Alteration (PIA; Fedo et al., 1995). Among these, the CIA, PIA and CIW are the most commonly used to interpret the weathering history of modern and ancient sediments (Harnois, 1988; Fedo et al. 1995; Tripathi and Rajamani, 1999; Saydam Eker, 2020).

* Corresponding author, e-mail: weronika.nadlonek@pgi.gov.pl

Received: Noevember 15, 2023; accepted: August 13, 2024; first published online: October 15, 2024

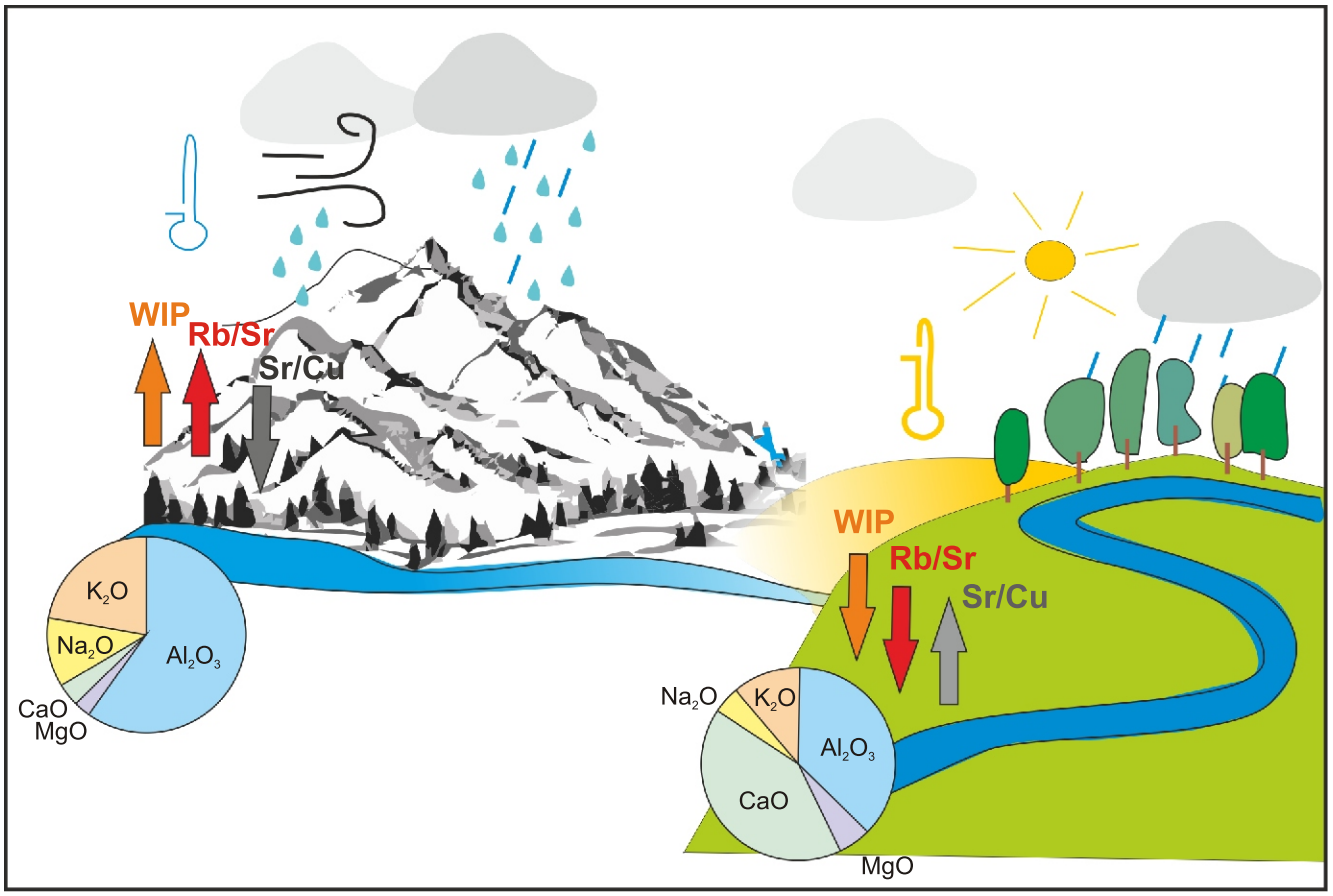

Graphical abstract

Element ratios of immobile to mobile elements, such as Rb/Sr and Sr/Cu, are also widely used to identify material origin, evaluate the degree of chemical weathering of the source rocks (Dasch, 1969; McLennan et al., 1993; Rahman et al., 2020, 2021), and determine the prevailing climatic conditions. Rubidium often occurs with potassium in silicate minerals, such as micas and potassium feldspars, due to the similarity of their ionic radii. Rubidium is released from these minerals in weathering processes and then adsorbed. Strontium, on the other hand, occurs in minerals containing calcium, in carbonate minerals, and in plagioclases (Liu et al, 2023; Ouyang et al., 2019). Rb/Sr ratios, particularly in lake sediments, reflect the relationship between physical and chemical weathering. Rb/Sr ratios decrease under drier conditions, while under the same conditions Sr/Cu ratios increase (Krzeszowska, 2019). During chemical weathering, the intensity of Sr leaching is more rapid than in the case of Rb (Nesbitt and Young, 1982). Furthermore, this ratio consequently increases with increasing CIA and vice versa (Ma et al., 2000).

Chemical weathering indices are widely applied in geology; in particular, they are used to evaluate the degree of weathering in soil profiles and to extract climatic and palaeoclimatic information from sedimentary records. In a series of studies on Chinese river relationships between the degree of silicate weathering intensity and climatic parameters, i.e. between temperature and runoff, were reported (Yang et al., 2004; Li and Yang, 2010; Shao et al., 2012). An example of using chemical weathering indices as climatic proxies in Poland comes from the study by Nadłonek and Bojakowska (2018), who emphasized the importance of lithology. These surveys were not supported by mineralogical research, a shortfall filled by this study.

However, the usefulness of weathering indices as climatic and palaeoclimatic proxies may be limited by several issues, including provenance control of sediment composition (e.g., Garzanti and Resentini, 2016), recycling and inheritance from previous sedimentary cycles (e.g., Borges et al., 2008), hydraulic effects and subsequent differentiation of grain size (e.g., Guo et al., 2018), uncertainties in separating CaO in carbonates or phosphates from Ca-silicate (e.g., Buggle et al., 2011), and biases related to various diagenetic processes, such as illitization (e.g., Buggle et al., 2011). Recent advances in the research on weathering indices in modern river sediments have raised the question about the role of lithology in the loss of soluble elements and the resulting ambiguity of CIA values (e.g., Chetelat et al., 2013). In addition to chemical processes, mechanical processes also regulate the weathering rate of rocks (Fletcher et al., 2006; Røyne et al., 2008).

Therefore, the purpose of this study was to: (1) estimate the chemical weathering indices for modern river sediments from two regions of Poland differing in climatic conditions, geological settings and topography, i.e. the Sudetes Mountains (the Kamienna and the Biała Lądecka rivers) and the Lublin Upland (the Chodelka and Żółkiewka rivers), (2) determine the main factors affecting the weathering of source rocks to a significant degree, (3) evaluate the usefulness of selected indices in assessing of the intensity of chemical weathering.

In particular, it was intended to answer the question of whether chemical weathering indices are affected by lithological effects and, hence, whether they can be used reliably as robust indicators of climate and palaeoclimate. Due to their complex geological settings and small catchment areas (<600 km^2) the rivers selected appear to be particularly suited for the purposes of this study.

DIFFERENCES IN THE RIVER SETTINGS

The scope of research included four selected rivers differing on a small (not global) scale in terms of climate, altitude, relief and lithology, but with similar total length.

The catchment area of the Kamienna lies within the Sudetes Mountains massif, which is part of a mountain-upland hydrogeological province. The Kamienna is a left-bank tributary of the Bóbr river, draining the eastern part of the Jizera Mountains, the western part of the Karkonosze Mountains and the southwestern part of the Jelenia Góra Valley. The catchment area is ~274.3 km^2 and the river length is ~32.4 km (Tarka and Olichwer, 2019). The source is located at an altitude of ~1120 m a.s.l. on the northern slopes of Mumlawski Wierch in the Karkonosze Mountains. It begins on the Zielony Klik peat bog. The channel of the Kamienna River has a natural character, however with hydrotechnical structures located along its course. The Szklarska Poręba II hydroelectric power plant is located in the river course headwaters. Below, in the town of Piechowice, there is a damming weir (Szklarska Poręba I). The land cover is mainly composed of forests.

The catchment area is located in the Sudetes Mountains climatic district, with diverse climatic conditions. The foothills have a temperate, cool, and humid climate shaped by air masses from the Atlantic. However, the climate in the Jizera Mountains and the Karkonosze Mountains is of typical mountain character, influenced by the orientation of the mountain barriers, elevation and terrain. The average annual temperature is 7–8°C. The annual rainfall is 650–750 mm (Bojakowska et al., 2004).

The Biała Lądecka is a right-bank tributary of the Nysa Kłodzka (Machajski and Olearczyk, 2010). Its catchment area covers 311.18 km^2 down to the mouth, and the river length is 52.29 km. The river's sources are located at 925.6 m above sea level. The sources of the Biała Lądecka are numerous streams located on the border of the Golden Mountains and the Bialskie Mountains (Eastern Sudetes). The main spring waters are two streams flowing down from the slope of Postawna: Biały Spław and Długi Spław. The upper part of the catchment area is largely forested and mountainous, while the lower part is submontane and is used for agriculture. Numerous tributaries feed the Biała Lądecka which is a river controlled at two water gauge sections (Lądek Zdrój and Żelazno). Numerous flood surges, with smaller or larger impacts, have been recorded on the Biała Lądecka.

The climate of the Biała Lądecka catchment area is moderate, with strong oceanic influences. Climatically, this area is divided into two separate zones: the Sudetes Foreland and the Sudetes Mountains. In the Foreland, winter is characterized by a daily temperature below 0°C and lasts for ~9–10 weeks, while in the mountains it lasts for 14–18 weeks. The growing season with a temperature above 5°C lasts for 30–32 weeks in the lowlands, while in the mountains, it lasts for 26–27 weeks. Summer with a temperature above 15°C lasts for 12–14 weeks in the low-pressure part and for 4–8 weeks in the Sudetes Mountains. The average annual temperature is 7°C (in Lądek Zdrój 6.5°C and decreases by ~1°C per 100 m elevation). The annual rainfall is 700–900 mm (Bobiński et al., 2004; Awdankiewicz et al., 2004).

The area of the Lublin Upland, containing the rivers studied, is characterized by features of a continental climate, in particular by moderately high temperatures. The precipitation recorded in this region varies significantly.

The Chodelka River is a right-bank tributary of the Vistula and is strongly meandering. Its length is 49.3 km, and the catchment area is 566.3 km^2. The source of the Chodelka is located at an altitude of 203.7 m a.s.l. in the area of the northern edge of the Urzędowskie hills. The valley is hilly, especially in the upper reaches of the river. Human activity has almost completely transformed the lower course of the river and the drainage systems within its valley. The changes relate to the artificial water circulation created for fishing and irrigation purposes. The nature of the outflow and changes in the water level of the lowest section of the Chodelka are influenced by fluctuations in the water level of the Vistula, which results in a backflow into the river valley of up to several kilometres during floods.

The catchment area of the Chodelka River is located in the transitional climate area between maritime and continental climates, in the so-called climatic zone of the great valleys (Bąk et al., 2010). The weather and climate are mainly affected by air masses blowing from the west. They are characterized by relatively mild winters, summers with little temperature range and a predominance of spring rainfall over autumn rainfall. It is a moderately warm climate. The average annual air temperature is 7.5–8°C, with the coldest month being January (average –4°C) and the warmest in July (+18°C). Precipitation reaches 550–600 mm/year, and the snow cover lasts on average 70–80 days a year in the area of the mouth of the Vistula River and up to 100 days in the river course headwater of the Chodelka River (Bąk et al., 2010; Andrzejewska-Kubrak et al., 2011).

The Żółkiewka is 39.17 km long and the total length of the catchment area is ~33 km. The left-bank side of the catchment area covers 148.97 km^2 and the right-bank side covers 67.28 km^2. The sources of the Żółkiewka are located at an altitude of 229.6 m a.s.l. There is a large, flat spring area in the basin. The Żółkiewka is fed by several small left-bank tributaries. Seasonal streams flow from numerous side valleys, gorges and ditches. In the valley, at the foot of the slopes, there are numerous permanent or seasonal springs, sometimes producing an abundant supply of water. It is characterized by a temperate continental climate. The catchment area is located in the Lublin-Zamość climatic region, which is shaped by the clashing influences of the continental and Atlantic climates. The average annual air temperature is 7.5–8°C, the average maximum temperature is 23°C and the average minimum temperature is –5°C. Precipitation values reach 500 to 700 mm/year (Mądry et al., 2011; Ślusarek et al., 2011).

GEOLOGY AND GEOMORPHOLOGY OF THE CATCHMENT AREAS

The Kamienna catchment area basement, along the entire section of the river, is composed of coarse and medium granites (Milewicz et al., 1989b; Appendix 1A), in the upper course – river equigranular, fine and medium granites and peats are also revealed at the surface. In the middle and upper courses of the river, mainly silts, sands and alluvial gravels are exposed. Fluvioglacial and deluvial sands and gravels, boulder clays, microgranites and gneisses also occur in the catchment area (Milewicz et al., 1989a; Appendix 2A).

The source of Kamienna River occurs on a peat plain at an altitude of over 1000 m a.s.l. The area of the river course's headwater typically contains flat surfaces of crystalline rocks and isolated rocks (Bobiński, 2015). In this section, the

Kamienna is surrounded mainly by mountain ridges. The middle section of the Kamienna catchment is separated from the upper course by tectonic fault-bounded long rock ridges (Appendix 3A). From this part to the mouth of the Kamienna River into the Bóbr River, catchments are formed primarily by accumulation terraces of the Kamienna River valleys and its tributaries, which cut through the undulating moraine plateau (Cymerman et al., 2011). In the north-western part of the catchment, there are denudational forms, such as slopes running parallel to the Kamienna River. Alluvial fans and river valleys are located at the foot of the slopes (Appendix 3A). The eastern side of the catchment area is dominated by ridges and rock peaks. Peat plains occur locally.

The basement of the Biała Lądecka catchment area consists mainly of metamorphic rocks (mica-schists, paragneisses, migmatites, eclogites) and igneous rocks, such as granites and granodiorites (Sawicki, 1988b; Appendix 1B). Mica-schists, paragneisses and migmatites, as well as eye-gneisses cover a large surface part of the catchment area. In the upper course of this river, besides shales, there are also amphibolites and igneous tonalites, while in the lower course, crystalline limestones, dolomitic marbles, sands, silts, alluvial gravels and loess deposits are exposed (Sawicki, 1988a; Appendix 2B).

In the river's upper reaches, there are mainly bare woods and hardwoods, and locally, flat areas. In this section, the Biała Lądecka River is surrounded by mountain ridges and denudation forms in the shape of long slopes (Appendix 3B; Cwojdziński, 2020). Numerous river valleys of various types are typical of the catchments. Highlands of undulose moraines characterize the middle and lower parts of the catchment area, and locally, there are loess covers and fragmentary outwash plains (Appendix 3B; Cymerman and Badura, 2019).

The bedrock of the Chodelka River is formed by limestone rocks, cherts, marls and chalks (Malinowski and Mojski, 1981b; Romanek, 2011b; Appendix 1C), while at the surface carbonate rocks are accompanied by glacial tills and aeolian deposits (Malinowski and Mojski, 1981a; Romanek, 2011a). In the upper course of the river and over the entire catchment area, glacial tills, peats, sandy and clay loesses, loams, clays and weathered sands, marls and chalk are exposed (Appendix 4A). In the central part of the catchment area, there are mainly sands, silts, alluvial sands and gravels, as well as flood plains and terraces, tills and aeolian sands. The estuary is dominated by silts, sands and gravels of river flood plains.

The upper reaches of the Chodelka River are dominated by overflood accumulation and erosion terraces surrounded by denudation plains and locally small areas of moraine plain (Appendix 5A; Marszałek, 2001). In the morphology of the terrain, these clearly are represented by flat surfaces. All forms extend to the lower course of the Chodelka River. In the lower and middle part of the catchment, there are areas of sand-covered plains, and in the vicinity of the catchment, there are loess covers (Kamiński, 2023). The lower course of the river is located within the wide Vistula valley (Appendix 5A).

The rocks in the Żółkiewka River basin are represented by sedimentary rocks (limestones, marls, calcareous cherts and chalks; Appendix 1D; Cieśliński and Rzechowski, 1997). At the surface of the catchment area there are mainly outcrops of calcareous rocks, younger loesses, sandy and clay loesses (Appendix 4B). In the upper reach of the river, silts, sands and gravels (also glaciofluvial) are exposed. However, deluvial sands and clays, and silts and sands of the high floodplain terrace, occur at the mouth of the Żółkiewka River flowing into the Wieprz River (Rzechowski, 1997). Flood terraces (accumulation) and over-flood terraces (accumulation and erosion) are an important element of the landscape of the Żółkiewka catchment area. The river valley cuts through the loess covers. Similarly to the Chodelka catchment area, there are also denudation plains in this area, especially near the upper reaches of the river, and slopes of plateau plains (Appendix 5B; Albrycht and Brzezina, 2000).

MATERIAL AND METHODS

The research was conducted on 30 sediment samples collected from two rivers in the Sudetes Mountains (the Kamienna, a left-bank tributary of the Bóbr, and the Biała Lądecka, a right-bank tributary of the Nysa Kłodzka) and two further rivers in the Lublin Upland (the Żółkiewka, a left-bank tributary of the Wieprz, and the Chodelka, a right-bank tributary of the Vistula).

Samples of alluvial sediments from the Holocene channel subfacies were collected with an aluminum scoop from the lower part of the meander outfall located underwater. Thirty samples, weighing ~0.5 kg each, were collected for geochemical analyses, together with twenty ~100-gram samples for mineralogical analyses.

The research area is shown on the map (Fig. 1), whilst the detailed location of sampling sites is given in the Appendicies 3 and 5. Sediment samples were collected at sites located along the entire length of the rivers, at relatively equal intervals, including the mouths of the rivers and their sources. The symbols used for the samples collected relate to their source rivers as follows: K – Kamienna, BL – Biała Lądecka, CH – Chodelka, Ż – Żółkiewka. Numbering starts at the source of the river and ends at the mouth.

WAVELENGTH DISPERSIVE X-RAY FLUORESCENCE SPECTROSCOPY (WD-XRF) AND INDUCTIVELY COUPLED PLASMA MASS SPECTROMETRY (ICP-MS)

Geochemical analyses of the main components (Al_2O_3, CaO, K_2O, MgO, and Na_2O) were carried out using Wavelength Dispersive X-Ray Fluorescence Spectroscopy (WD-XRF). The expanded uncertainty of the results was provided with the assumed 95% probability level and the expansion factor $k = 2$. The detection limits were 0.05–0.40%, 0.01–0.20%, 0.01–0.60%, 0.01–0.60% and 0.01–0.40% for Al_2O_3, CaO, K_2O, MgO, and Na_2O, respectively. For determination by WD-XRF, before preparing a glass for testing, one gram of air-dried sample was ground to a grain size < 0.063 mm and roasted with the addition of 4.87 g of flux – mixture: 34% $LiBO_2$ (lithium metaborate) + 66% $Li_2B_4O_7$ (lithium tetraborate) at a temperature of ~1000°C.

The resulting amounts of oxides were used to calculate the WIP, V, CIA, CIW, and PIA values (molecular proportions of oxides) according to the following formulae:

$$WIP = \left(\frac{2Na_2O}{0.35} + \frac{MgO}{0.9} + \frac{2K_2O}{0.25} + \frac{CaO}{0.7}\right) 100 \quad \text{(Parker, 1970)}$$

$$V = \frac{Al_2O_3}{MgO + CaO + Na_2O + K_2O} \quad \text{(Vogt, 1927)}$$

$$CIA = \frac{Al_2O_3}{Al_2O_3 + CaO + Na_2O + K_2O} 100 \quad \text{(Nesbitt and Young, 1982)}$$

$$CIW = \frac{Al_2O_3}{Al_2O_3 + CaO + Na_2O} 100 \quad \text{(Harnois, 1988)}$$

Fig. 1. Location of the research areas

$$PIA \quad \frac{Al_2O_3 \quad K_2O}{Al_2O_3 \quad CaO+Na_2O \quad K_2O} \quad 100$$

(Fedo et al., 1995)

Measurements of Cu, Sr, and Rb content were conducted by Inductively Coupled Plasma Mass Spectrometry (ICP-MS). The expanded uncertainty of the results was 25% with an assumed 95% confidence level and expansion factor k=2. The air-dried test samples were ground to a grain size <0.063 mm and dissolved in open vessels, in a mixture of inorganic acids with hydrofluoric acid (HF), on a heating plate at a temperature not exceeding 220°C. One gram of each sample was weighed and placed in a Teflon container. Concentrated nitric acid HNO_3 was added and the sample was evaporated on the hotplate to wet salts. Then, concentrated HNO_3 and HF were added and evaporated on a hot plate into wet salts until the sample was completely dissolved. After that, concentrated HNO_3 and concentrated $HClO_4$ (perchloric acid) were added and the sample was evaporated to an almost dry state. The walls of the vessel were rinsed with distilled water and evaporated to wet salts. It was then dissolved in the hot state in 5 ml of concentrated HNO_3. The contents of the vessel were transferred to a polyethylene or polypropylene bottle, filtered and topped up with deionized water to a mass of 50 g. All geochemical analyses were made in the PGI-NRI Chemical Laboratory in Warsaw.

STATISTICAL ANALYSES

The statistical parameters (minimum, maximum, median, mean, and geometric mean) for the oxide contents and the weathering indices were calculated using *Statistica* software.

SCANNING ELECTRON MICROSCOPE (SEM-EDS)

Mineralogical analyses (SEM-EDS analyses) of polished mounts, prepared from the sediment grains, sieved through nylon sieves with a mesh size of 2.0 mm, and then sprayed with carbon threads, were undertaken using a *HITACHI SU3500* scanning electron microscope. The accelerating voltage was set to 15 kV, the working distance was 10 mm, and the spot size (probe current) set to 70%; analysis time varied from 5 to 15 seconds. The chemical composition of minerals was obtained by semi-quantitative analysis with a Thermo Scientific UltraDry Compact EDS Detector.

X-RAY DIFFRACTION (XRD)

The mineral composition of the alluvial sediments was determined by X-ray diffraction at the Institute of Earth Sciences (University of Silesia in Katowice). The XRD analyses were car-

ried out on samples of alluvial material that were not separated into fractions. The samples were powdered using an *X'Pert Pro MPD PW3040/60* diffractometer made by PANalytical, Almelo, the Netherlands. The measurement conditions were as follows: an acceleration voltage of 45 kV, a current of 40 mA, and 0.01 step sizes between the angles of 2.5 and 65° 2 , and a 300 s measurement time per step. The data obtained were processed using HighScore+ software (version 4.9) and the ICSD database.

SIEVE ANALYSIS – GRANULOMETRIC COMPOSITION ANALYSES

The dried sample material was sifted through sieves with specific mesh sizes and then the percentage of grains remaining on subsequent sieves relative to the total weight of the tested sample was calculated. To analyze the river sediments, a set of sieves was used with mesh sizes: 1.5 mm, 1.00 mm, 0.63 mm, 0.5 mm, 0.25 mm, 0.1 mm and 0.056 mm.

The standard classification of siliciclastic rocks was applied in the study. To shorten the description of the facies, symbols used in this work were applied according to Miall (1977) and Zieliński (1995); only the textural code for clay (Y) comes from Widera et al. (2019).

RESULTS

GEOCHEMICAL ANALYSES

All calculated statistical parameters are shown in Table 1. The Al_2O_3 content in the sediments of the Kamienna and Biała Lądecka rivers ranges from 10.23 to 13.47% (Table 1; Appendix 6). CaO contents vary in the range of 0.25–3.24%, K_2O between 2.39 and 4.79%, MgO from 0.23 to 2.79% and Na_2O from 1.69 to 2.23% (Table 1). Standard deviation values for all the oxides from the Sudetes Mountains rivers are in the range of 0.16 to 0.81, while the coefficient of variation (CV) values range from 7 to 74 (Table 1). The copper content in sediments of the Kamienna and Biała Lądecka rivers ranges from 4.05 to 31.65 ppm, the rubidium from 101.58–257.13 ppm, and the strontium from 47.30 to 239.70 ppm. Standard deviation values for Cu, Rb, and Sr from the Sudetes Mountains sediments range from 6.34 to 50.24, whereas the coefficient of variation (CV) values range from 29 to 43 (Table 1).

The Al_2O_3 content in the sediments of the Lublin Upland rivers (Chodelka and Żółkiewka) ranges from 1.07–6.21%, Ca (0.43–7.91%), K_2O (0.40–1.70%), MgO (0.01–0.68%) and Na_2O (0.15–0.62%). The copper content in sediments of the

Table 1

Statistical parameters of oxides (%) and elements content (ppm) in the river sediments

Oxide/ element	$\bar{x}$	GM	Me	Min	Max	s	CV
SUDETES MOUNTAINS Kamienna and Biała Lądecka rivers n=15							
Al_2O_3	11.09	11.06	10.92	10.23	13.47	0.81	7
CaO	1.06	0.87	0.89	0.25	3.24	0.76	72
K_2O	3.53	3.46	3.31	2.39	4.79	0.71	20
MgO	0.87	0.72	0.71	0.23	2.79	0.64	74
Na_2O	1.95	1.94	1.94	1.69	2.23	0.16	8
Cu	15.42	14.02	15.47	4.05	31.65	6.34	41
Rb	174.91	167.97	157.39	101.58	257.13	50.24	29
Sr	110.85	102.60	102.90	47.30	239.70	47.90	43
LUBLIN UPLAND Chodelka and Żółkiewka rivers n = 15							
Al_2O_3	2.51	2.10	1.58	1.07	6.21	1.63	65
CaO	2.21	1.58	1.19	0.43	7.91	2.01	91
K_2O	0.78	0.70	0.52	0.40	1.70	0.41	52
MgO	0.22	0.12	0.12	0.01	0.68	0.21	93
Na_2O	0.32	0.28	0.23	0.15	0.62	0.17	52
Cu	16.79	5.27	3.98	1.83	181.97	45.81	273
Rb	27.16	23.88	18.44	13.20	63.42	15.30	56
Sr	86.57	65.86	52.80	23.90	230.90	69.19	80

$\bar{x}$ – mean, GM – geometric mean, Me – median, Min – minimum, Max – maximum, s – standard deviation, CV – coefficient of variation

Chodelka and Żółkiewka ranges from 1.83 to 181.97 ppm, the rubidium from 13.20 to 63.42 ppm, and the strontium from 23.90 to 230.90 ppm (Table 1). The standard deviation values for oxides analyzed in the Lublin Upland river sediments range from 0.17 to 2.01 with the coefficient of variation values varying from 52 to 93. The Cu content in sediments of the Chodelka and Żółkiewka ranges from 1.83 to 181.97 ppm, Rb from 13.20 to 63.42 ppm, and Sr from 23.90 to 230.90 ppm. Standard deviation values for Cu, Rb, and Sr from the Lublin Upland river sediments fell between 15.30 and 69.19, with the coefficient of variation (CV) values ranging from 56 to 273 (Table 1).

The highest WIP values, ranging from 54.55 to 60.52, were observed in the Kamienna river in the Sudetes Mountains, while values between 46.18 and 58.23 were reported from sediments of the Biała Lądecka (Table 2). The lowest WIP values were measured in the rivers in the Lublin Upland. Values ranging from 6.97 to 34.54 in the Chodelka and from 6.12 to 30.42 were recorded in the Żółkiewka.

The V index values in the Sudetes Mountains ranged from 2.21 to 3.80 for the Kamienna and from 0.86 to 2.24 for the Biała Lądecka. Values between 0.31 and 2.30 were observed in the Chodelka and values between 0.52 and 1.20 were seen in the Żółkiewka (Table 2).

The CIA values in the sediments of the Kamienna ranged from 53.89 to 56.75. Similar values were found in the sediments of the Biała Lądecka (49.07–58.23). Lower values were observed in the Chodelka (19.64–56.48) and Żółkiewka (28.42–42.27). A similar trend is noticeable in the case of the CIW and PIA.

The most common values of the indices analyzed (percentile range 25–75) in the sediments of the rivers investigated are illustrated in the boxplots (Fig. 2).

The range of WIP, CIA, CIW, and PIA values for the sediments of the rivers from the Sudetes Mountains is much narrower compared to those of the Lublin Upland (Fig. 2). The V index values for Sudetes Mountains' rivers are higher than these

Table 2

Statistical parameters of the chemical weathering indices

Index	$\bar{x}$	GM	Me	Min	Max	s	CV
Kamienna River n = 7							
WIP	56.67	56.64	56.25	54.55	60.52	1.96	3
V	2.84	2.78	2.70	2.21	3.80	0.60	21
CIA	54.98	54.97	54.73	53.89	56.75	1.00	2
CIW	71.41	71.35	70.59	67.95	75.75	2.97	4
PIA	59.33	59.28	58.48	57.05	63.54	2.43	4
Rb/Sr	3.11	2.98	2.70	2.20	4.87	1.00	32
Sr/Cu	7.13	6.72	5.94	4.22	11.68	2.71	38
Biała Lądecka River n = 8							
WIP	49.87	49.77	49.88	46.18	58.23	3.41	7
V	1.81	1.74	2.03	0.86	2.24	0.48	27
CIA	55.77	55.70	56.63	49.07	58.23	2.84	5
CIW	66.61	66.42	68.60	55.08	71.03	5.15	8
PIA	58.77	58.62	59.59	48.81	62.87	4.31	7
Rb/Sr	1.04	0.97	1.13	0.42	1.35	0.35	34
Sr/Cu	8.30	7.89	8.14	4.11	12.76	2.71	33
Chodelka River n = 8							
WIP	15.77	13.65	12.14	6.97	34.54	9.53	60
V	0.84	0.68	0.66	0.31	2.30	0.65	77
CIA	32.27	30.65	31.79	19.64	56.48	11.62	36
CIW	37.30	34.89	36.67	20.83	68.97	15.26	41
PIA	27.82	25.46	25.20	15.75	60.16	14.20	51
Rb/Sr	0.44	0.39	0.41	0.17	0.72	0.20	45
Sr/Cu	14.67	9.65	14.01	0.27	23.47	7.51	51
Żółkiewka River n = 7							
WIP	15.92	13.60	13.05	6.12	30.42	9.48	60
V	0.83	0.80	0.83	0.52	1.20	0.21	25
CIA	35.03	34.75	33.93	28.42	42.27	4.77	14
CIW	40.13	39.71	38.07	31.34	50.99	6.39	16
PIA	30.25	29.82	29.84	23.48	38.25	5.61	19
Rb/Sr	0.34	0.33	0.32	0.27	0.55	0.10	29
Sr/Cu	17.83	16.77	19.66	6.81	22.28	5.50	31

$\bar{x}$ – mean, GM – geometric mean, Me – median, Min – minimum, Max– maximum, s – standard deviation, CV – coefficient of variation

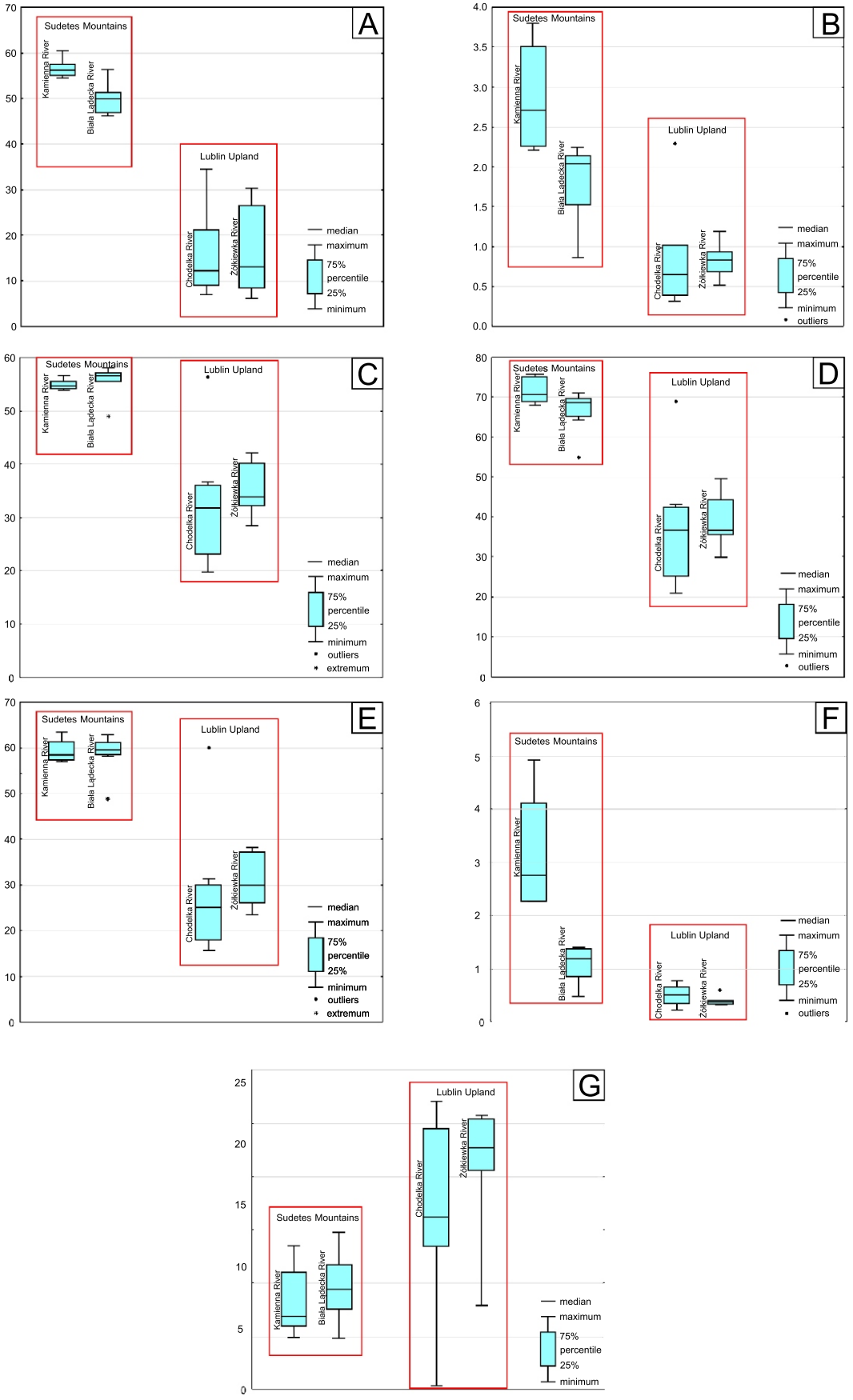

Fig. 2. Boxplots of chemical weathering indices in the sediments of the rivers investigated: A – WIP, B – V, C – CIA, D – CIW, E – PIA, F – Rb/Sr, G – Sr/Cu

of the Lublin Upland, but are within a small range of from 0.31–3.80 for all rivers. In the Sudetes Mountains, the range of Rb/Sr index values was significantly higher than in the Lublin Upland, in contrast to Sr/Cu index values.

GRAIN SIZE ANALYSIS

Sieve analysis showed the predominance of coarse and medium sands in the Kamienna and Biała Lądecka rivers (Table 3). Fine and medium-grained sands dominate the Lublin Upland river sediments, while in the case of the Chodelka, in the middle and upper reaches, mainly fine sands, silts, and clays prevail. These sediments are also characterized by a better degree of sorting.

MINERALOGY OF RIVER SEDIMENTS

In the 20 samples investigated, as indicated in the Appendix 6, observations were made using a scanning electron microscope and fine fraction was analyzed on an XRD diffractometer. This enabled the identification of minerals and differences in chemical composition in the river sediments from the Sudetes Mountains and the Lublin Upland. In rivers from the Sudetes Mountains, the grains are more sharp-edged, with variables forms and types of fractions (Fig. 3 and Table 3), whilst in the case of the Lublin Upland, they are better coated and composed of finer fractions. In both cases of the sources of the rivers, the grains are more irregular and as they approach their mouths, sediment components become more regular and coated (for example see Fig. 3G, H).

Sieve analysis showed the predominance of coarse and medium sands in the Kamienna and Biała Lądecka rivers. Fine and medium-grained sands dominate the Lublin Upland river sediments, while in the case of the Chodelka, in the middle and upper reaches, mainly fine sands, silts, and clays prevail. These sediments are also characterized by better sorting.

The minerals found in the Kamienna River are mainly quartz, plagioclases (mainly albite), and potassium feldspars (mainly microcline) (Fig. 3 and Table 4). Mica grains (both biotite and muscovite) are also common. Clay minerals are represented by illite and chlorites (clinochlore). Additionally, single grains of amphibole, garnet, zircon, monazite and ilmenite are present. A similar composition was observed in the sediments from the Biała Lądecka, with more frequent appearance of Fe oxides and dolomite grains. Quartz is the dominant component of sediments from the Lublin area, reaching concentrations of up to 95 and 96% for the Chodelka River and Żółkiewka River, respectively (Table 4). Additionally, plagioclases and potassium feldspars occur. In the case of the Żółkiewka River, a significant amount of calcite was also detected. The sediments of both rivers differ significantly in terms of accessory and trace minerals: garnets, ilmenites, Fe oxides, and magnetite characterize the Chodelka River, while Fe oxides, Ti oxides, titanite, Fe phosphates, epidotes, and amphiboles were found in samples from the Żółkiewka River.

DISCUSSION

FACTORS INFLUENCING THE CHEMICAL WEATHERING PROXIES

The rate of chemical weathering results from several factors, including lithology, climate, tectonic relief, physical erosion, vegetation, soil development, hydrology, and human activity and susceptibility to erosion (White and Blum, 1995; Bahlburg and Dobrzinski, 2011; Bouchez et al., 2012; Shao et al., 2012; Babechuk et al., 2014; Batista et al., 2017; Kidane et al., 2019; Li et al., 2021). Primary material is transported along the rivers, depending on the river flow rate, which is influenced by, among other factors, the slope angle, rainfall intensity and the type of soil particles. The weathering rate decreases with increasing grain size, but the overall weathering is determined also by the rate of dissolution along grain boundaries (depending on grain density). In coarse-grained sediments, the detachment into smaller grains has a significant contribution to the total weathering (Israeli and Emmanuel, 2018). As grain size decreases, the chemical weathering rate increases. In the riverbeds of the mountain rivers with significant inclination and increased rainfall, sediment transport is more dynamic, as shown by the dominance of the sandy fraction with a low gravel content (Table 3). In the case of the mountain rivers, the basin is composed of very resistant metamorphic rocks, however the steep and/or deforested slopes result in the weathered rocks being more exposed to erosion (Agaj and Bytyqi, 2022). Rivers in the Lublin Upland area are characterized by a lower intensity of flow (Wyżga and Ciszewski, 2010), due to the lesser slope of the terrain. Granulometric and mineralogical analysis of the river sediments collected (both from the mountain and upland rivers) indicates the transport of material in suspension. Fine fractions (sand, silt and clay) were probably transported for longer distances, while the transport distance of fine gravels found in the samples from the Kamienna and Biała Lądecka was shorter.

Hydrotechnical development and incorrect regulation of riverbeds (Ashraf et al., 2016), may cause hydrodynamic balance disorders (Korpak et al., 2023). River regulation destroys the natural structure of the bed and changes the nature of water flow. Rapid water surges then destroy the bed structure, reinforcing the erosion process, while limiting the size of flood areas causes an increase in the peak of individual runoff (Škarpich et al., 2013; Korpak et al., 2023). As a result, the overall weathering rate arises from the combined effects of chemical and physical processes together with anthropogenic processes (Israeli and Emmanuel, 2018). In the case of mountain rivers, the basin is composed of metamorphic rocks which are very resistant; however, steep and/or deforested slopes make weathered rocks more exposed to soil erosion (Agaj and Bytyqi, 2022).

CHEMICAL WEATHERING PROXIES IN DIFFERENT BASINS

This study was conducted to isolate specific causes influencing weathering rates using the rivers of the Sudetes Mountains and the Lublin Upland as case studies. Those basins differ significantly in terms of geology and climate, making them ideal case study areas for discussing the factors bearing on the weathering and the usefulness of weathering indices in small regional-scale studies. Variations in weathering indices in the rivers investigated suggest that different drainage basins result in different scenarios, regulated by various driving forces.

The average CIW (66.61–71.41), PIA (58.77–59.33), and CIA (54.98–55.77) indices of the sediments from the Sudetes rivers, along with an Rb/Sr ratio >1, indicate more intensive weathering at their sources than in the case of the Lublin Upland (e.g., Hossain et al., 2017; Abedini and Khosravi, 2022). This could be attributed to the high runoffs from mountainous areas and the continuous erosion of soils in these regions. In the mountains (Biała Lądecka and Kamienna catchments) where elevated annual precipitations (650–900 mm) and average temperatures 7–8° occur, the intensity of chemical weathering is stronger than in the Lublin Upland, where the average

Table 3

Granulometric composition of the studied river sediments based on sieve analyses, the grain-size content is expressed in % by weight

Granulometry											
Sample number	Lithofacies	Gravel fraction (mm)	Sand & silt fractions (mm)								Type of dominante sediment
		>2.00	1.25	1.00	0.63	0.5	0.25	0.1	0.056	<0.056	
K1	S	0.90	3.4	1.7	16.2	1.9	63.0	12.8	0.6	0.5	Medium sand
K2	S	0.2	16.7	6.0	19.2	10.5	32.6	13.9	0.7	0.4	Coarse sand and medium sand
K5	S	0.4	11.0	10.3	37.7	16.4	23.7	0.8	0.1	0.1	Coarse sand and medium sand
K6	S	1.1	23.1	17.9	35.6	9.2	8.8	3.6	0.4	0.3	Coarse sand
K7	S	0.9	14.7	12.2	27.2	0.3	38.9	4.7	0.4	0.7	Coarse sand and medium sand
BL1	S	3.0	13.7	8.6	19.1	4.9	41.3	8.4	0.5	0.5	Coarse sand and medium sand
BL2	S	1.0	4.2	3.7	20.3	21.8	43.2	5.2	0.3	0.2	Coarse sand and medium sand
BL4	S	0.3	3.6	7.4	41.1	7.9	13.3	22.8	2.2	1.6	Coarse sand
BL7	S	4.1	12.9	7.9	20.7	11.5	26.9	13.1	1.9	1.1	Coarse sand and medium sand
BL8	S	1.8	10.2	8.2	26.2	0.3	43.7	8.2	0.9	0.5	Coarse sand and medium sand
CH1	S	0.3	1.2	0.7	3.9	7.2	57.9	24.8	2.1	1.8	Medium sand and fine sand
CH2	S	0.5	0.5	0.5	2.3	4.1	47.4	40.2	2.8	1.7	Medium sand and fine sand
CH5	FY	0.0	0.7	0.3	4.3	3.7	12.7	22.7	26.7	29.0	Silt and clay
CH7	S	0.2	0.6	0.3	1.9	3.8	52.2	36.2	2.8	1.9	Medium sand and fine sand
CH8	SF	0.0	0.2	0.2	1.2	0.2	25.0	42.1	16.2	15.1	Fine sand and silt
Ż1	S	0	0.05	0.1	1.1	1.8	74.8	21.5	0.2	0.5	Medium sand and fine sand
Ż2	SF	0.2	0.6	0.2	1.8	0.1	66.8	22.1	3.6	4.6	Medium sand and fine sand
Ż4	SF	0.1	0.2	1.1	2.9	0.2	39.0	38.7	7.8	10.2	Medium sand and fine sand
Ż6	SF	0.1	0.3	0.5	4.4	0.3	49.5	24.7	7.5	12.7	Medium sand and fine sand
Ż7	SF	0.5	2.3	2.1	12.4	12.2	41.2	18.7	3.8	6.8	Medium sand and fine sand

Codes of the textural elements of the various lithofacies after Miall (1977), Zieliński (1995) and Widera et al., (2019): S – sand, F – silt, Y – clay

annual precipitation is 500–700 mm and temperatures are 7.5–8°. Fluvial sediments in areas with elevated annual precipitations and lower average annual temperatures are characterized by a higher degree of weathering. In the Sudetes Mountains, ~45% of the region's area is characterized by moderate and strong erosion. This is caused by significant relative altitudes, steep slopes and high annual rainfall (Nowocień, 2008; Dąbek et al., 2018). Erosion processes have been substantially intensified as a result of anthropogenic impacts involving, for instance, changes of the river character and drainage system, alteration of land relief, agriculture and deforestation (Krzemień et al., 2015; Dąbek et al., 2018). Furthermore, the exposed source rocks in the Sudetes Mountains catchments are more readily weathered and transported by the rivers.

The CIA is used to evaluate the degree of mineral transformation into clay minerals. Sediments with high WIP and CIW values may originate from immature precursor sediments and characterize first-cycle deposits, whilst sediments with low WIP values may have been derived from mature sediments (Kamp and Leake, 1985; Wang et al., 2014). The values are higher for sediments and sedimentary rocks which are composed of complex mineralogical mixtures (carbonates, phyllosilicates and phosphates). The CIA value is useful when it reflects the progressive alteration of potassium feldspar and plagioclase to clay minerals during rock weathering (Nesbitt and Young, 1982; Zhou et al., 2017). The classification of CIA values (50–60) according to Nesbitt and Young (1982) suggests that all the sediments studied are much less weathered by comparison with other climatic zones. The topography of the land surface is also an important factor influencing the intensity of weathering, which shapes the energy of water flow in watercourses and the type of sedimentary material found in the river bed. The sources of material transported in rivers vary. Some of it comes directly from the bottom or edges of the riverbed as a result of bottom and side erosion (Ballio et al., 2010). Material brought by a tributary may have a similar character. Moreover, the slopes of valleys, from where sediment can be directly delivered to the riverbed through surface flows and mass movements, are an

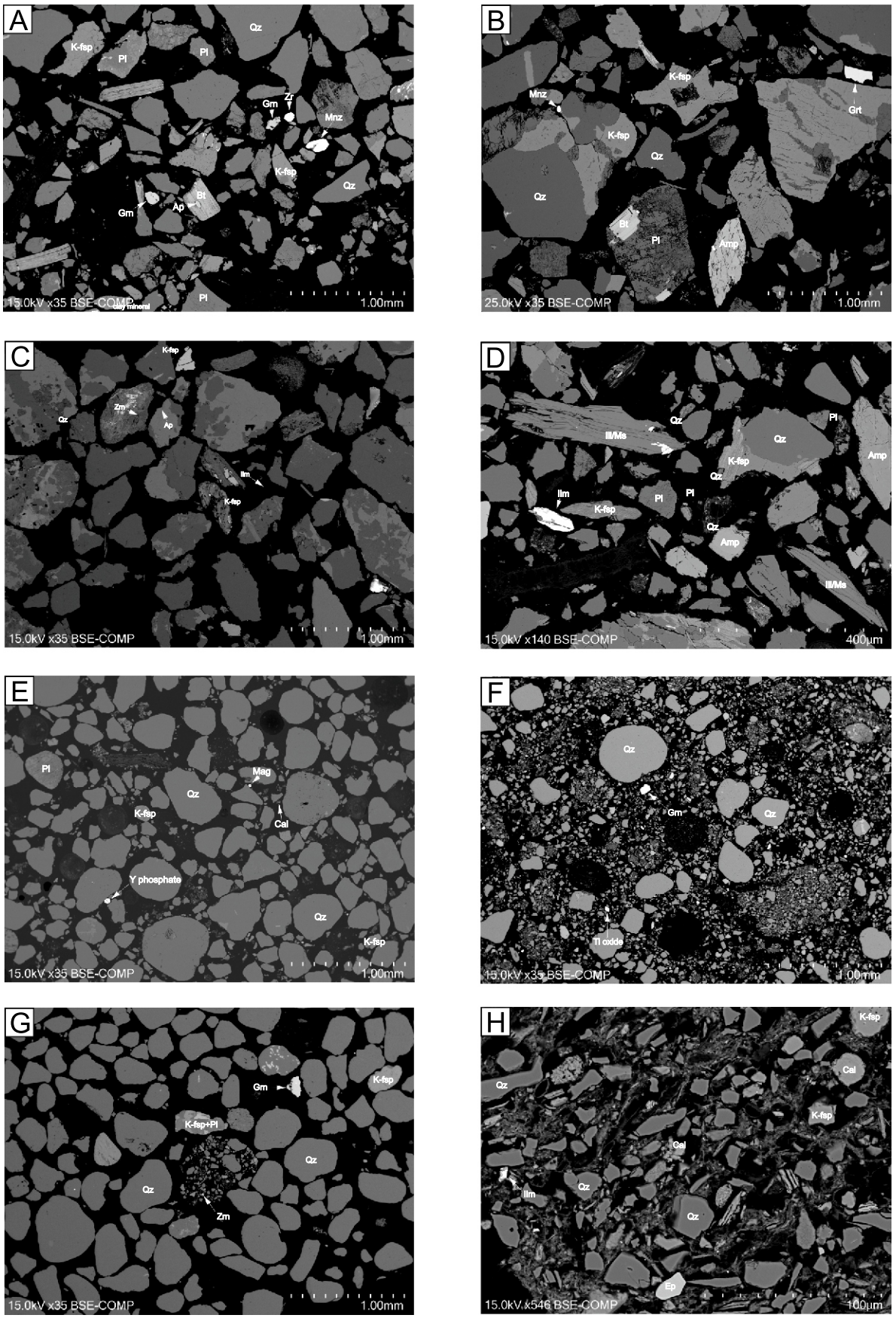

Fig. 3. SEM images of selected river sediments (A – K1, B – K6, C – BL1, D – BL8, E – CH1, F – CH8, G – Z1, H – Z6)

Abbreviations for the names of rock-forming minerals according to Whitney and Evans (2010)

Table 4

XRD analysis of river sediment samples (% by weight)

Samples	Minerals											
	Quartz	Micro-cline	Albite	Biotite	Illite	Clino-chlore	Muscovite	Ortho-clase	Horn-blende	Magnesio-hornblende ferrian	Calcite	Rutile
K1	64.5	17	14.5	0.5	2.5	1	0	0	0	0	0	0
K7	45.5	25.5	19	0	3.5	2	4.5	0	0	0	0	0
BL1	53.5	22.5	15.1	0	1.5	2.5	3	0.5	1	0	0	0
BL8	56.5	10	25.5	0	1	2	0.5	0	0	4.5	0	0
CH1	95	2	2	0	0	1	0	0	0	0	0	0
CH8	79	9	8	0	2	1.5	0	0	0.5	0	0	0
Ż1	96.2	0	3.2	0	0	0	0	0	0	0	0.3	0
Ż7	89.5	2.5	3	0.5	0	0	0	0	0.5	0	4	0.3

important source area (Ilinca, 2021). These relationships reflect the results obtained for rivers in mountain and upland areas. Furthermore, the kind of facies in the river system also plays an important role in the length and dynamics of transport (Yan et al., 2017). In the bottoms of river beds in mountain rivers with significant inclination and increased rainfall, sediment transport is more dynamic, while the floodplains and terraces in most sampling sites in the Lublin Upland are characterized by lower rates and intensities of flow (Wyżga and Ciszewski, 2010).

Decreasing CIA, CIW, and PIA values should coincide with increasing WIP and V values and vice versa (Shao et al., 2012). However, in this study, there is a lack of such correlation which could suggest that the WIP should be considered as an indicator of provenance, specifically recycling, rather than weathering (Garzanti and Resentini, 2016). The WIP is very sensitive to quartz content (e.g., quartz/feldspar ratios), which is closely related to sediment recycling and source lithology. The Chemical Index of Alteration (CIA) and Weathering Index of Parker (WIP) values (Figs. 4 and 5) showed the prevalence of intense physical weathering in mountain river basins (Panwar and Chakrapani, 2016). The lack of correlation between these indicators is likely due to the influence of sediment grain size on CIA values (Li and Yang, 2010). Changes in grain size impact sediment composition (Panwar and Chakrapani, 2016). Mud contains a high quantity of clay minerals and sands are more feldspathic in nature and rich in quartz. Intense chemical weathering results in the formation of fine-grained secondary minerals (Nesbitt et al., 1996).

At the scale of the basins of the rivers studied, the weathering indices show a relatively stable distribution from the sources of the rivers though the middle courses, to the mouths. Therefore, the sediments in suspension at the river sources were not necessarily subjected to less intense chemical weathering than sediments transported in the middle course or located close to the mouths (Chetelat et al., 2013), which is related to the flow rate. This is observed not only in the values for chemical weathering, but also in the sediment fractions (Table 3) and mineralogical compositions (Table 4) of the material studied.

Further geochemical studies on trace elements led to conclusions regarding climatic conditions. In the Lublin area, a warmer and drier climate is clearly reflected by lower Rb/Sr ratios (0.17–0.72) than in the Sudetes Mountains (0.42–4.87) (Table 2) which indicates that sediments from Chodelka and Zółkiewka were not subjected to intense chemical weathering (Rahman et al., 2020) and have low aluminum contents (Oni and Olatunji, 2017). In mountain rivers, Rb/Sr usually exceeds 1, which indicates intense weathering (McLennan et al., 1993; Armstrong-Altrin et al., 2019) and the presence of illite in the sediment (Chaudhuri and Brookins, 1979). This is corroborated in the mineral composition of the sediments studied (Table 4). Illite and chlorite dominate where erosion is mainly physical (Chamley, 1989). Low Sr/Cu ratios are typical of a warm humid climate, whereas high Sr/Cu ratios indicate a hot climate (Jia et al., 2013). In the Lublin area, a warmer and drier climate is clearly reflected by higher Sr/Cu (median for Chodelka – 14.01 and Żółkiewka – 19.66) and lower Rb/Sr ratios, respectively (Table 2). The higher Rb/Sr ratio (median for Biała Lądecka –1.13 and Kamienna – 2.70) and lower Sr/Cu (median for Biała Lądecka –8.14 and Kamienna – 5.94) in mountain areas suggest increased precipitation.

COMPARISON OF CHEMICAL WEATHERING PROXIES IN DIFFERENT BASINS

The WIP values are in the range from 0 to 100 (the higher values are typical for less weathered rocks). In our study, the mean values for the rivers studied are relatively low, also when compared with results obtained from chemical weathering indices in the study by Nadłonek and Bojakowska (2018), where large catchments (Vistula and Odra) were investigated and there were many samples. WIP values are much higher in small streams in the Sudetes Mountains (mean in Odra River basin 3.2, compared to the Sudetes Mountains 49.87–56.67; Table 5). The mean value for the Vistula River basin was 5.1, whilst in the Lublin Upland rivers, the values ranged from 15.77 to 15.92 (Table 2). When comparing these results with Chojnicki's (2022) results from the depth of 0–40 cm, pertaining to alluvial soils of the middle Vistula and Żuławy (Vistula delta) the results are higher (19–31.9) than in the Lublin Upland, but much lower than in the Sudetes Mountains.

The values of the V index obtained in all the rivers studied (mean from 0.83 to 2.84), which serve to determine the maturity of the residual sediments, were higher than in the Vistula and Odra basins (0.4 and 0.8 respectively), but the difference is not excessive; however, in the alluvial soils of the middle Vistula valley, V values were approximately in the range 1.8–2.3 and in the soils of Żuławy from 2.0 to 2.9 (Chojnicki, 2022). The values obtained corroborate stronger weathering in the Sudetes Mountains. The stronger chemical weathering during the transport of sediments also results from a higher content of mobile elements (Table 1).

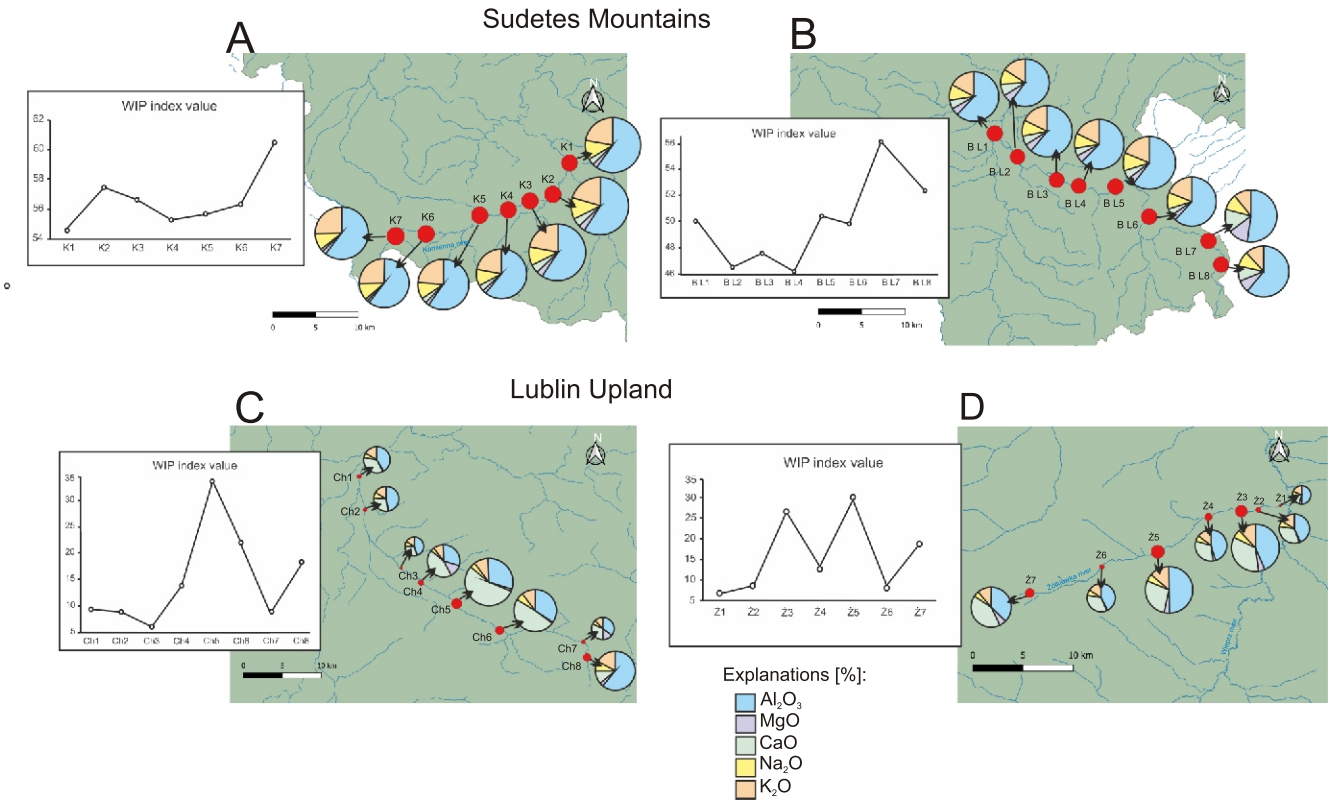

Fig. 4. WIP index values and element oxide content for selected river sediments (K – Kamienna, BL – Biała Lądecka, CH – Chodelka, Ż – Żółkiewka)

The different sizes of the diagrams show the changes in WIP values along the rivers' courses

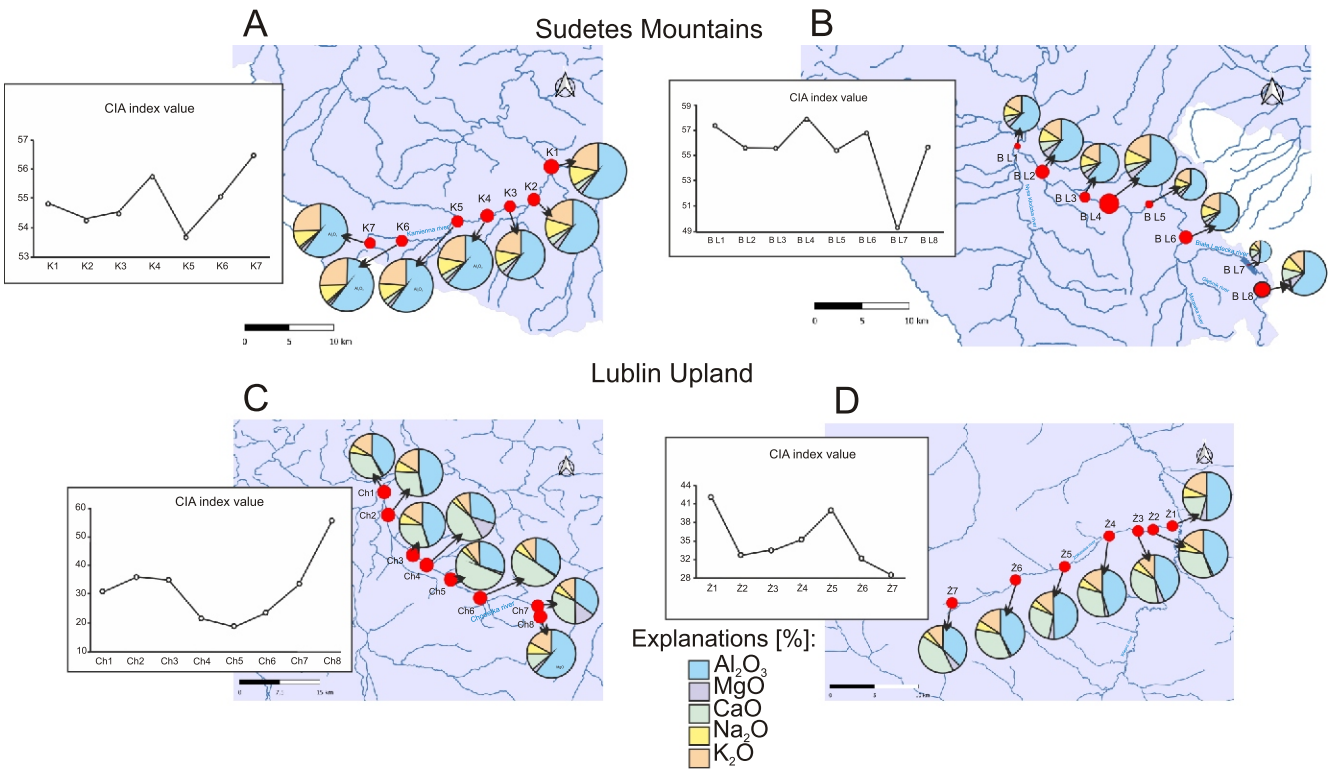

Fig. 5. CIA index values and element oxide content for selected river sediments (K – Kamienna, BL – Biała Lądecka, CH – Chodelka, Ż – Żółkiewka)

The different sizes of the diagrams show changes in the WIP values along the rivers' courses

Table 5

Comparison of mean values of chemical weathering indices in different basins

Chemical weathering index	Sudetes Mountains rivers[1]	Lublin Upland rivers[1]	Odra catchment[2]	Vistula catchment[2]	Alluvial soils of middle Vistula valley[3]	Alluvial soils of Żuławy[3]
WIP	49.87–56.67	15.77–15.92	3.2	5.1	19.0–31.9	24.2–31.5
V	1.81–2.84	0.83–0.84	0.8	0.4	1.8–2.3	2.0–2.9
CIA	54.98–55.77	32.27–35.03	45	27.6	57.9–65.8	60.0–76.0
CIW	66.61–71.41	37.30–40.13	48.4	28.9	67.3–76.3	70.2–87.2
PIA	58.77–59.33	27.82–30.25	44.9	26.2	47.7–60.3	53.2–72.4

References: [1] – actual research, [2] – (Nadłonek and Bojakowska, 2018), [3] – (Chojnicki, 2022)

The situation changed in the case of the CIA, CIW and PIA. These results are much lower in large basins, comparing values from the Vistula catchment with Lublin Upland rivers and from the Odra catchment with Sudetes rivers (Nadłonek and Bojakowska, 2018), but in a similar range when compared with alluvial soils of the middle Vistula valley and Żuławy (CIA: 57.9–76, CIW: 67.3–87.2 and PIA: 47.7–72.4; Chojnicki, 2022).

The values obtained of standard deviation (<100) and coefficient of variation (<200) indicate a moderately homogenous distribution in sediments and in their lithogenic source (Tables 1 and 2). An exception is the coefficient of variation for copper (a potentially toxic element) in the Lublin Upland river, which suggests that it is of anthropogenic origin.

FUTURE OUTLOOK

Due to the problem of climate change – rising average temperatures, and more frequent sudden, sometimes extreme, weather phenomena – scientists are conducting extensive research and observations on changes in average temperatures. While these changes are inevitable, they can be predicted and the human impact on them can be limited. One method for estimating the rate of temperature change (increase and decrease) is the use of chemical weathering indices, which provide information regarding different climate conditions. To compare past and present situations, it would be valuable to examine changes in indicators over time. One interesting approach could involve comparing the results of chemical weathering indices calculated for sediment samples using data from the Geochemical Atlas of Poland (Lis and Pasieczna, 1995) with current samples taken at the same locations, or even extending the research and attempting a similar analysis for the data included in the Geochemical Atlas of Europe (Salminen, 2005). The topic discussed in this preliminary study is complex and still raises many questions. The limitations in the interpretation are related to the small sample population, very small extent of study area and short length of the rivers. Moreover, the topic is relatively underdeveloped in Poland and neighbouring countries (most case studies come from China), which makes it difficult to compare results from the same climatic zone. In the future, it would be worthwhile to delve deeper into the detailed mineralogy of river sediments, land relief and changes in natural environment caused by humans.

CONCLUSIONS

1. The values obtained of chemical weathering indices (V, CIA, CIW, PIA) indicate a clearly higher intensity of weathering processes in the Sudetes Mountains.
2. Trace element contents (Rb, Sr, Cu) reflect the climate well, but other chemical weathering indices used seem to be more sensitive to the mineral composition and properties of the grains.
3. More intense chemical weathering took place in a mountainous region with elevated annual precipitation and lower annual temperatures.
4. Although the climate controls the chemical weathering process, other factors, such as basement geology, grain size, mineralogical composition of sediments, physical erosion and human activity affect its intensity.
5. The presence of illite and clinochlorite, as well as the WIP and CIA values obtained for the rivers of the Sudetes Mountains, indicate a dominance of physical weathering.

Acknowledgements. The authors thank prof. I. Bojakowska for her constructive and detailed remarks and we are very grateful for all comments by prof. A. Wysocka as well as by other, anonymous reviewers. This research was in whole funded by the National Science Centre, Poland [Grant no. 2022/06/X/ST10/00716]. We are very grateful to dr T. Krzykawski from the Institute of Earth Sciences (Faculty of Natural Sciences) of the University of Silesia for carrying out X-ray diffraction analyses. For the purpose of Open Access, the author has applied a CC-BY public copyright license to any Author Accepted Manuscript (AAM) version arising from this submission.

Data Availability. The geochemical data of analyses conducted by ICP-MS and WD-XRF methods used in this study are enclosed in the Appendicies to the manuscript and also posted in the open data repository RepOD: https://doi.org/10.18150/VLQMCI.

REFERENCES

Abedini, A., Khosravi, M., 2022. Geochemical constraints on the Zola-Chay river sediments, NW Iran: implications for provenance and source-area weathering. Arabian Journal of Geosciences, **15**, 1515; https://doi.org/10.1007/s12517-022-10822-y

Agaj, T., Bytyqi, V., 2022. Analysis of soil erosion risk in a river basin – a case study from Hogoshti River Basin (Kosovo). Ecological Engineering & Environmental Technology, **23**: 162–171; https://doi.org/10.12912/27197050/143380

Albrycht, A., Brzezina, R., 2000. Objaśnienia do szczegółowej mapy geologicznej Polski w skali 1: 50 000; Arkusz Żółkiewka (824) (in Polish). Państwowy Instytut Geologiczny, Warszawa.

Andrzejewska-Kubrak, K., Gabryś-Godlewska, A., Kozłowska, O., Kwecko, P., Miecznik, J., Walentek, I., Wojciechowska, K., 2011. Objaśnienia do mapy geośrodowiskowej Polski 1:50 000, Arkusz Chodel (784) (in Polish). Państwowy Instytut Geologiczny, Warszawa.

Armstrong-Altrin, J.S., Botello, A.V., Villanueva, S.F., Soto, L.A., 2019. Geochemistry of surface sediments from the north western Gulf of Mexico: implications for provenance and heavy metal contamination. Geological Quarterly, **63** (3): 522–538; https://doi.org/10.7306/gq.1484

Ashraf, F. B., Haghighi, A. T., Marttila, H., Klřve, B., 2016. Assessing impacts of climate change and river regulation on flow regimes in cold climate: a study of a pristine and a regulated river in the sub-arctic setting of Northern Europe. Journal of Hydrology, **542**: 410–422; https:// doi.org/10.1016/j.jhydrol.2016.09.016

Awdankiewicz, H., Bobiński. W., Lis, J., Pasieczna, A., Wołkowicz, S., Bujakowska, K., Hrybowicz, G., Wojciechowska, K., 2004. Objaśnienia do mapy geośrodowiskowej Polski 1:50 000, Arkusz Kłodzko (901) (in Polish). Państwowy Instytut Geologiczny, Warszawa.

Babechuk, M., Widdowson, M., Kamber B.S., 2014. Quantifying chemical weathering intensity and trace element release from two contrasting basalt profiles, Deccan Traps, India. Chemical Geology, **363**: 56–75; https:// doi.org/10.1016/j.chemgeo.2013.10.027

Bahlburg, H., Dobrzinski, N., 2011. A review of the Chemical Index of Alteration (CIA) and its application to the study of Neoproterozoic glacial deposits and climate transitions. Geological Society of London, Memoirs, **36**: 81–92; https://doi.org/10.1144/M36.6

Ballio, F., Brambilla, D., Giorgetti, E., Longoni, L., Papini, M., Radice, A., 2010. Evaluation of sediment yield from valley slopes: A case study. WIT Transactions on Engineering Sciences, **67**: 149–160; https:// doi.org/10.2495/DEB100131

Batista, P.V.G., Silva, M.L.N., Silva, B.P.Ch., Curi, N., Bueno, I.T., Júnior, F.W.A., Davies, J., Quinton, J., 2017. Modelling spatially distributed soil losses and sediment yield in the upper Grande River Basin – Brazil. Catena, **157**: 139–150; https://doi.org/10.1016/j.catena.2017.05.025

Bąk, B., Szeląg, A., Bojakowska, I., Kwecko, P., Tomassi-Morawiec, H., Wojciechowska, K., 2010. Objaśnienia do mapy geośrodowiskowej Polski 1:50 000, Arkusz Kazimierz Dolny (746) (in Polish). Państwowy Instytut Geologiczny, Warszawa.

Ber, A., 2013. Objaśnienia do Szczegółowej Mapy Geologicznej Polski 1:50 000, Nałęczów (747) (in Polish). Państwowy Instytut Geologiczny, Warszawa.

Bobiński, W., 2015. Objaśnienia do szczegółowej mapy geologicznej Polski 1:50 000, Arkusz Jakuszyce (831) i Szklarska Poręba (831) (in Polish). Państwowy Instytut Geologiczny, Warszawa.

Bobiński, W., Bojakowska, I., Gawlikowska, E., Kłonowski, M., Koźma, J., Lis, J., Pasieczna, A., Wołkowicz, S., 2004. Objaśnienia do mapy geośrodowiskowej Polski 1:50 000, Arkusz Kłodzko (901) (in Polish). Państwowy Instytut Geologiczny, Warszawa.

Bojakowska, I., Gawlikowska, E., Koźma, J., Lis, J., Różański, P., Ordzik, K., Pasieczna, A., Sobol, L., Wołkowicz, S., 2004. Objaśnienia do mapy geośrodowiskowej Polski 1:50 000, Arkusz Jelenia Góra (795) (in Polish). Państwowy Instytut Geologiczny, Warszawa.

Borges, J.B., Huh, Y., Moon, S., Noh, H., 2008. Provenance and weathering control on river bed sediments of the eastern Tibetan Plateau and the Russian Far East. Chemical Geology, **254**: 52–72; https:// doi.org/10.1016/j.chemgeo.2008.06.002

Bouchez, J., Gaillardet, J., Lupker, M., Louvat, P., France Lanord, C., Maurice, L., Armijos, E., Moquet J.-S., 2012. Floodplains of large rivers: Weathering reactors or simple silos? Chemical Geology, **332–333**: 166–184; https://doi.org/10.1016/j.chemgeo.2012.09.032

Buggle, B., Glaser, B., Hambach, U., Gerasimenko, N., Marković, S., 2011. An evaluation of geochemical weathering indices in loess–paleosol studies. Quaternary International, **240**: 12–21; https://doi.org/10.1016/j.quaint.2010.07.019

Chamley, H., 1989. Clay Sedimentology. Springer, Berlin.

Chaudhuri, S., Brookins, D.G., 1979. The Rb Sr systematics in acid-leached clay minerals. Chemical Geology, **24**: 231–242; https://doi.org/10.1016/0009-2541(79)90125-6

Chetelat, B., Liu, C.-Q., Wang, Q., Zhang, G., 2013. Assessing the influence of lithology on weathering indices of Changjiang river sediments. Chemical Geology, **359**: 108–115; https://doi.org/10.1016/j.chemgeo.2013.09.018

Chojnicki, J., 2022. Chemical weathering of the middle Vistula and Żuławy (Vistula delta) alluvial soils. Soil Science Annual, **73**, 157349; https://doi.org/10.37501/soilsa/157349

Cieśliński, S., Rzechowski, J., 1997. Mapa Geologiczna Polski B – mapa bez utworów czwartorzędowych w skali 1:200 000 Arkusz Chełm, Horodło (in Polish). Polska Agencja Ekologiczna S.A., Warszawa.

Cwojdziński, S., 2020. Objaśnienia do szczegółowej mapy geologicznej Polski w skali 1: 50 00, Arkusz Złoty Stok (902) (in Polish). Państwowy Instytut Geologiczny, Warszawa.

Cymerman, Z., Badura, J., 2019. Objaśnienia do szczegółowej mapy geologicznej Polski w skali 1: 50 00, Arkusz Kłodzko (901) (in Polish). Państwowy Instytut Geologiczny, Warszawa.

Cymerman, Z., Cwojdziński, S., Kozdrój, W., 2011. Objaśnienia do szczegółowej mapy geologicznej Polski w skali 1: 50 00, Arkusz Jelenia Góra (in Polish). Państwowy Instytut Geologiczny, Warszawa.

Dąbek, P., Żmuda, R., Szczepański, J., Ćmielewski, B., 2018. Evaluation of water soil erosion processes in forest areas in the Western Sudetes using terrestrial laser scanning and GIS tools. E3S Web of Conferences, **44**, 00026; https://doi.org/10.1051/e3sconf/20184400026

Dasch, E.J., 1969. Strontium isotopes inweathering profiles, deep-sea sediments,and sedimentary rocks. Geochimica et Cosmochimica Acta, **33**: 1521–1552; https://doi.org/10.1016/0016-7037(69)90153-7

Dupré, B., Dessert, C., Oliva, P., Goddéris, Y., Viers, J., François, L., Millot, R., Gaillardet, J., 2003. Rivers, chemical weathering and Earth's climate. Comptes Rendus Geoscience, **335**: 1141–1160; https://doi.org/10.1016/j.crte.2003.09.015

Fedo, C.M., Nesbitt, H.W., Young, G.M., 1995. Unraveling the effects of potassium metasomatism in sedimentary rocks and paleosols, with implications for paleoweathering conditions and provenance. Geology, **23**: 921–924; https://doi.org/10.1130/0091-7613(1995)023<0921:UTEOPM>2.3.CO;2

Fletcher, R.C., Buss, H.L., and Brantley, S.L., 2006. A spheroidal weathering model coupling porewater chemistry to soil thicknesses during steady-state denudation. Earth and Planetary Science Letters, **244**: 444–457; https://doi.org/10.1016/j.epsl.2006.01.055

Garzanti, E., Resentini, A., 2016. Provenance control on chemical indices of weathering (Taiwan river sands). Sedimentary Geology, **336**: 81–95; https://doi.org/10.1016/j.sedgeo.2015.06.013

Guo, Y., Yang, S., Su, N., Li, C., Yin, P., & Wang, Z., 2018. Revisiting the effects of hydrodynamic sorting and sedimentary recycling on chemical weathering indices. Geochimica et Cosmochimica Acta, **227**: 48–63; https://doi.org/10.1016/j.gca.2018.02.015

Harasimiuk M., Henkiel A., Król T., 1988. Objaśnienia do szczegółowej mapy geologicznej Polski 1:50 000, Krasnystaw (725) (in Polish). Państwowy Instytut Geologiczny, Warszawa.

Harnois, L., 1988. The CIW index: a new Chemical Index of Weathering. Sedimentary Geology, **55**: 319–322; https://doi.org/10.1016/0037-0738(88)90137-6

Hossain, H.M.Z., Kawahata, H., Roser, B.P., Sampei, Y., Manaka, T., Otani, S., 2017. Geochemical characteristics of modern river sediments in Myanmar and Thailand: implications for provenance and weathering. Geochemistry, **77**: 443–458; https://doi.org/10.1016/j.chemer.2017.07.005

Ilinca, V., 2021. Using morphometrics to distinguish between debris flow, debris flood and flood (Southern Carpathians, Romania). Catena, **197**: 104982; https://doi.org/10.1016/j.catena.2020.104982

Israeli, Y., Emmanuel, Simon., 2018. Impact of grain size and rock composition on simulated rock weathering. Earth Surface Dynamics. **6**: 319–327; https:// doi.org/10.5194/esurf-6-319-2018

Jia, J., Liu, Z., Bechtel, A., Strobl, S.A.I., Sun, P., 2013. Tectonic and climate control of oil shale deposition in the Upper Cretaceous Qingshankou Formation (Songliao Basin, NE China). International Journal of Earth Sciences, **102**: 1717–1734; https://doi.org/10.1007/s00531-013-0903-7

Kamiński, M., 2023a. Objaśnienia do szczegółowej mapy geologicznej Polski 1:50 000, Arkusz Kazimierz Dolny (746) (in Polish). Państwowy Instytut Geologiczny, Warszawa.

Kamiński, M., 2023b. Objaśnienia do szczegółowej mapy geologicznej Polski 1:50 000, Opole Lubelskie (783) (in Polish). Państwowy Instytut Geologiczny, Warszawa.

Kamp, P.C., Leake, B.E., 1985. Petrography and geochemistry of feldspathic and mafic sediments of the northeastern Pacific margin. Transaction of the Royal Society of Edinburgh. Earth Sciences, **76**: 411–449; https://doi.org/10.1017/S0263593300010646

Kidane, M., Bezie, A., Kesete, N., Tolessa, T., 2019. The impact of land use and land cover (LULC) dynamics on soil erosion and sediment yield in Ethiopia. Heliyon, **5**, e02981; https://doi.org/10.1016/j.heliyon.2019.e02981

Korpak, J., Radecki-Pawlik, A., Lenar-Matyas, A., 2023. Spatial and temporal variability of the morphodynamics of a regulated mountain river. Journal of Hydrology, **622**, Part A, 129719; https://doi.org/10.1016/j.jhydrol.2023.129719

Krzemień, K., Gorczyca, E., Sobucki, M., Liro, M., Lyp, M., 2015. Effects of environmental changes and human impact on the functioning of mountain river channels, Carpathians, southern Poland. Annals of Warsaw University of Life Sciences – SGGW, Land Reclamation, **47**: 249–260; https://doi.org/10.1515/sggw-2015-0029

Krzeszowska, E., 2019. Geochemistry of the Lublin Formation from the Lublin Coal Basin: Implications for weathering intensity, palaeoclimate and provenance. International Journal of Coal Geology, **216**, 103306; https://doi.org/10.1016/j.coal.2019.103306

Li, C., Yang, S., 2010. Is chemical index of alteration (CIA) a reliable proxy for chemical weathering in global drainage basins? American Journal of Science, **310**: 111–127; https://doi.org/10.2475/02.2010.03

Li, J., Liu, S., Shi, X., Zhang, H., Cao, P., Li, X., Pan, H.-J., Khokiattiwong, S., Kornkanitnan, N., 2021. Applicability and variability of chemical weathering indicators and their monsoon-controlled mechanisms in the Bay of Bengal. Frontiers in Earth Science, **9**, 633713; https://doi.org/10.3389/feart.2021.633713

Lis, J., Pasieczna A., 1995. Atlas geochemiczny Polski w skali 1:2 500 000 (in Polish). Państwowy Instytut Geologiczny, Warszawa.

Lisicki S., 2008. Objaśnienia do szczegółowej mapy geologicznej Polski 1:50 000, Arkusz Mirsk (794) (in Polish). Państwowy Instytut Geologiczny, Warszawa.

Liu, L., Yu, K., Li, A., Zhang, C., Wang, L., Liu, X., Lan, J., 2023. Weathering intensity response to climate change on decadal scales: a record of Rb/Sr ratios from Chaonaqiu Lake sediments, Western Chinese Loess Plateau. Water, **15**, 1890; https://doi.org/10.3390/w15101890

Ma, Y., Liu, C., Huo, R., 2000. Strontium isotope systematics during chemical weathering of granitoids: importance of relative mineral weathering rates. Journal of Conference Abstracts, **5**, 657.

Machajski, J., Olearczyk, D., 2010. Analiza możliwości energetycznego wykorzystania istniejącego piętrzenia w km 10+100 biegu rzeki Biała Lądecka (in Polish). Infrastruktura i Ekologia Terenów Wiejskich, (08/1).

Malinowski, J., Mojski, J.E., 1981a. Mapa geologiczna polski A – mapa utworów powierzchniowych w skali 1:200 000 Arkusz Lublin (in Polish). Wyd. Geol., Warszawa.

Malinowski, J., Mojski, J.E., 1981b. Mapa geologiczna polski B – mapa bez utworów czwartorzędowych w skali 1:200 000 Arkusz Lublin (in Polish). Wyd. Geol., Warszawa.

Marszałek, S., Albrycht, A., Bula, S., 1991. Objaśnienia do szczegółowej mapy geologicznej Polski 1:50 000, Niedrzewica (785) (in Polish). Państwowy Instytut Geologiczny, Warszawa.

Marszałek, S., 2001. Objaśnienia do szczegółowej mapy geologicznej Polski 1:50 000, Arkusz Chodel (784) (in Polish). Państwowy Instytut Geologiczny, Warszawa.

Maslov, A.V., Podkovyrov, V.N., 2023. Chemical weathering indices and their use for paleoclimatic reconstructions (on the example of the Vendian–Lower Cambrian section of Podolsk Transnistria). Lithology and Mineral Resources, **58**: 213–234; https://doi.org/10.1134/S0024490222700043

Mądry, S., Bojakowska, I., Kwecko, P., Miecznik, J., Wojciechowska, K., 2011. Objaśnienia do mapy geośrodowiskowej Polski 1:50 000, Arkusz Krasnystaw (825) (in Polish). Państwowy Instytut Geologiczny, Warszawa.

McLennan, S.M., Hemming, S., McDaniel, D.K. and Hanson, G.N., 1993. Geochemical approaches to sedimentation, provenance, and tectonics. GSA Special Paper, **284**: 21–40; https://doi.org/10.1130/SPE284-p21

Miall, A.D., 1977. A rewiew of the braided-river depositional environment. Earth-Science Reviews, **13**: 1–62; https://doi.org/10.1016/0012-8252(77)90055-1

Milewicz, J., Szałamacha, J., Szałamacha, M., 1989a. Mapa geologiczna Polski A – mapa utworów powierzchniowych w skali 1:200 000 Arkusz Jelenia Góra (in Polish). Wyd. Geol., Warszawa.

Milewicz, J., Szałamacha, J., Szałamacha, M., 1989b. Mapa geologiczna Polski B – mapa bez utworów czwartorzędowych w skali 1:200 000 Arkusz Jelenia Góra (in Polish). Wyd. Geol., Warszawa.

Morawski W., 2020. Objaśnienia do szczegółowej mapy geologicznej Polski 1:50 000, Arkusz Stronie Śląskie (934) i Bielice (935). (in Polish). Państwowy Instytut Geologiczny, Warszawa.

Nadłonek, W., Bojakowska, I., 2018. Variability of chemical weathering indices in modern sediments of the Vistula and Odra Rivers (Poland). Applied Ecology And Environmental Research, **16**: 2453–2473; https://doi.org/10.15666/aeer/1603_24532473

Neall, V.E., 1977. Genesis and weathering of andosols in Taranaki, New Zealand. Soil Science, **123**: 400–408.

Nesbitt, H.W., Young, G.M., 1982. Early Proterozoic climates and plate motions inferred from major element chemistry of lutites. Nature, **299**: 715–717.

Nesbitt, H.W., Young, G.M., McLennan, S.M., Keays, R.R., 1996. Effect of chemical weathering and sorting on the petrogenesis of siliciclastic sediments, with implication for provenance studies. Journal of Geology, **104**: 525–542; https://doi.org/10.1086/629850

Nowocień, E., 2008. Selected problems of soil erosion in Poland. Studia i Raporty IUNG – PIB, **10**: 9–38.

Oni, S.O., Olatunji, A.S., 2017. Depositional environments signatures, maturity and source weathering of Niger Delta sediments from an oil well in southeastern Delta State, Nigeria. Eurasian Journal of Soil Science, **6**: 259–274; https://doi.org/10.18393/ejss.297245

Ouyang, S., Ashraf, M.A., Hung, Y.T., 2019. Application of Rb/Sr ratio in paleo-climate inversion. Nature Environment and Pollution Technology, **18** (Special Issue): 1713–1718.

Panwar, S., Chakrapani, G.J., 2016. Seasonal variability of grain size, weathering intensity, and provenance of channel sediments in the Alaknanda River Basin, an upstream of river Ganga, India. Environmental Earth Sciences, **75**, 998; https://doi.org/10.1007/s12665-016-5815-y

Parker, A., 1970. An index of weathering for silicate rocks. Geological Magazine, **107**: 501–504

Perri, F., 2018. Reconstructing chemical weathering during the Lower Mesozoic in the Western-Central Mediterranean area: a review of geochemical proxies. Geological Magazine, **155**: 944–954; https://doi.org/10.1017/S0016756816001205

Price, J.R., Velbel, M.A., 2003. Chemical weathering indices applied to weathering profiles developed on heterogenous felsic metamorphic parent rocks. Chemical Geology, **202**: 397–416; https://doi.org/10.1016/j.chemgeo.2002.11.001

Rahman, M.A., Das, S.C., Pownceby, M.I., Tardio, J., Alam, M.S., Zaman, M.N., 2020. Geochemistry of Recent Brahmaputra River sediments: provenance, tectonics, source area weathering and depositional environment. Minerals, **10**, 813; https://doi.org/10.3390/min10090813

Rahman, M.M., Hasan, M.F., Hasan, A.S.M.M., Alam M.S., Biswas P.K., Zaman M.N., 2021. Chemical weathering, provenance, and tectonic setting inferred from recently deposited sediments of Dharla River, Bangladesh. Journal of Sedimentary Environments, **6**: 73–91; https://doi.org/10.1007/s43217-020-00046-z

Romanek, A., 2011a. Mapa geologiczna Polski A – mapa utworów powierzchniowych w skali 1:200 000 Arkusz 59 – Sandomierz (M-34-X) (in Polish). L. Marks. MŚ, Warszawa.

Romanek, A., 2011b. Mapa geologiczna Polski B – mapa bez utworów czwartorzędowych w skali 1:200 000 Arkusz 59 – Sandomierz (M-34-X) (in Polish). MŚ, Warszawa.

Røyne, A., Jamtveit, B., Mathiesen, J., Malthe-Sørenssen, A., 2008. Controls on rock weathering rates by reaction-induced hierarchical fracturing. Earth and Planetary Science Letters, **275**: 364–369; https://doi.org/10.1016/j.epsl.2008.08.035

Rzechowski, J., 1997. Mapa geologiczna Polski A – mapa utworów powierzchniowych w skali 1:200 000 Arkusz Chełm, Horodło (in Polish). Polska Agencja Ekologiczna S.A., Warszawa.

Salminen, R., 2005. Geochemical Atlas of Europe, Part I. Geological Survey of Finland, Espoo.

Sawicki, L., 1988a. Mapa geologiczna Polski A – mapa utworów powierzchniowych w skali 1:200 000 Arkusz Kłodzko (in Polish). Wyd. Geol., Warszawa.

Sawicki, L., 1988b. Mapa geologiczna Polski B – mapa bez utworów czwartorzędowych w skali 1:200 000 Arkusz Kłodzko (in Polish). Wyd. Geol., Warszawa.

Saydam Eker, C., 2020. Geochemical differences between bed and terrace sediments of the Harşit Stream (NE Turkey): implications for mixed source rocks, weathering and mass transfer. Yerbilimleri, **41**: 1–29; https://doi.org/10.17824/yerbilimleri.684511

Shao, J., Yang, S., Li, C., 2012. Chemical indices (CIA and WIP) as proxies for integrated chemical weathering in China: Inferences from analysis of fluvial sediments. Sedimentary Geology, **265–266**: 110–120; https://doi.org/10.1016/j.sedgeo.2012.03.020

Sharma, A., Rajamani, V., 2000. Major element, REE, and other trace element behavior in amphibolite weathering under semiarid conditions in southern India. Journal of Geology, **108**: 487–496; https://doi.org/10.1086/314409

Škarpich, V., Hradecký, J., Dušek, R., 2013. Complex transformation of the geomorphic regime of channel in the forefield of the Moravskoslezské Beskydy Mts.: Case study of the Morávka River (Czech Republic). Catena, **111**: 25–40; https://doi.org/10.1016/j.catena.2013.06.028

Ślusarek, W., Kwecko, P., Miecznik, J., Wojciechowska, K., 2011. Objaśnienia do mapy geośrodowiskowej Polski 1:50 000, Arkusz Żółkiewka (824) (in Polish). Państwowy Instytut Geologiczny, Warszawa.

Tarka, R., Olichwer, T., 2019. Zmiany przepływu rzecznego w Polsce Południowo-Zachodniej i jego związek z Oscylacją Północnoatlantycką (in Polish). In: NAO – jej istota, przyczyny i konsekwencje (eds. A. Staszyńska, M. Błaś and K. Migała): 63–74. IGiRR Uniwersytet Wrocławski, Stowarzyszenie Klimatologów Polskich, Wrocław.

Tripathi, J.K., Rajamani, V., 1999. Geochemistry of the loessic sediments on Delhi Ridge, eastern Thar Desert, Rajasthan: implications for exogenic processes. Chemical Geology, **155**: 265–278; https://doi.org/10.1016/S0009-2541(98)00168-5

Vogt, T., 1927. Sulitjelma field's geology and petrographyi (in Norwegian with English summary). Norges Geologiske Undersokelse, **121**: 1–560.

Wang, Y., Long, X., Wilde, A.A., Xu, H., Sun, M., Xiao, W., 2014. Provenance of Early Paleozoic metasediments in the central Chinese Altai: Implication for tectonic affinity of the Altai-Mongolia terrane in the Central Asian Orogenic Belt. Lithos, **210–211**: 57–68; https://doi.org/10.1016/j.lithos.2014.09.026

White, A.F., Blum, A.E., 1995. Effects of climate on chemical weathering in watersheds. Geochimica et Cosmochimica Acta, **59**: 1729–1747; https://doi.org/10.1016/0016-7037(95)00078-E

Whitney, D.L., Evans, B.W., 2010. Abbreviations for names of rock-forming minerals. American Mineralogist, **95**: 185–187; https://doi.org/10.2138/am.2010.3371

Widera, M., Chomiak, L., Zieliński, T., 2019. Sedimentary facies, processes and paleochannel pattern of an anastomosing river system: an example from the Upper Neogene of Central Poland. Journal of Sedimentary Research, **89**: 487–507; https://doi.org/10.2110/jsr.2019.28

Wyżga, B., Ciszewski D., 2010. Hydraulic controls on the entrapment of heavy metal-polluted sediments on a floodplain of variable width, the upper Vistula River, southern Poland. Geomorphology, **117**: 272–286; https://doi.org/10.1016/j.geomorph.2009.01.016

Yan, Q., Iwasaki, T., Stumpf, A., Belmont, P., Parker, G., Kumar, P., 2017. Hydrogeomorphological differentiation between floodplains and terraces. Earth Surface Processes and Landforms, **43**: 218–228; https://doi.org/10.1002/esp.4234

Yang, J., Cawood, P.A., Du, Y., Li, W., Yan, J., 2016. Reconstructing Early Permian tropical climates from chemical weathering indices. GSA Bulletin, **128**: 739–751; https://doi.org/10.1130/B31371.1

Yang, S., Jung, H.S., Li, C., 2004. Two unique weathering regimes in the Changjiang and Huanghe drainage basins: geochemical evidence from river sediments. Sedimentary Geology, **164**: 19–34; https://doi.org/10.1016/j.sedgeo.2003.08.001

Zhou, L., Friis, H., Yang, T., Nielsen, A.N., 2017. Geochemical interpretation of the Precambrian basement and overlying Cambrian sandstone on Bornholm, Denmark: Implications for the weathering history. Lithos, **286-287**: 369–387; https://doi.org/10.1016/j.lithos.2017.06.019

Zieliński, T., 1995. Kod litofacjalny i litogenetyczny – konstrukcja i zastosowanie (in Polish). Badania osadów czwartorzędowych. Wybrane metody i interpretacja wyników: 221–234. WGiSR UW, Warszawa.

APPENDIX 1

Geological revealed maps of the studied catchments areas: A – Kamienna river, B – Biała Lądecka river, C – Chodelka river, D – Żółkiewka river according to Malinowski and Mojski (1981b); Sawicki (1988b); Milewicz et al. (1989b); Cieśliński and Rzechowski (1997) and Romanek (2011b)

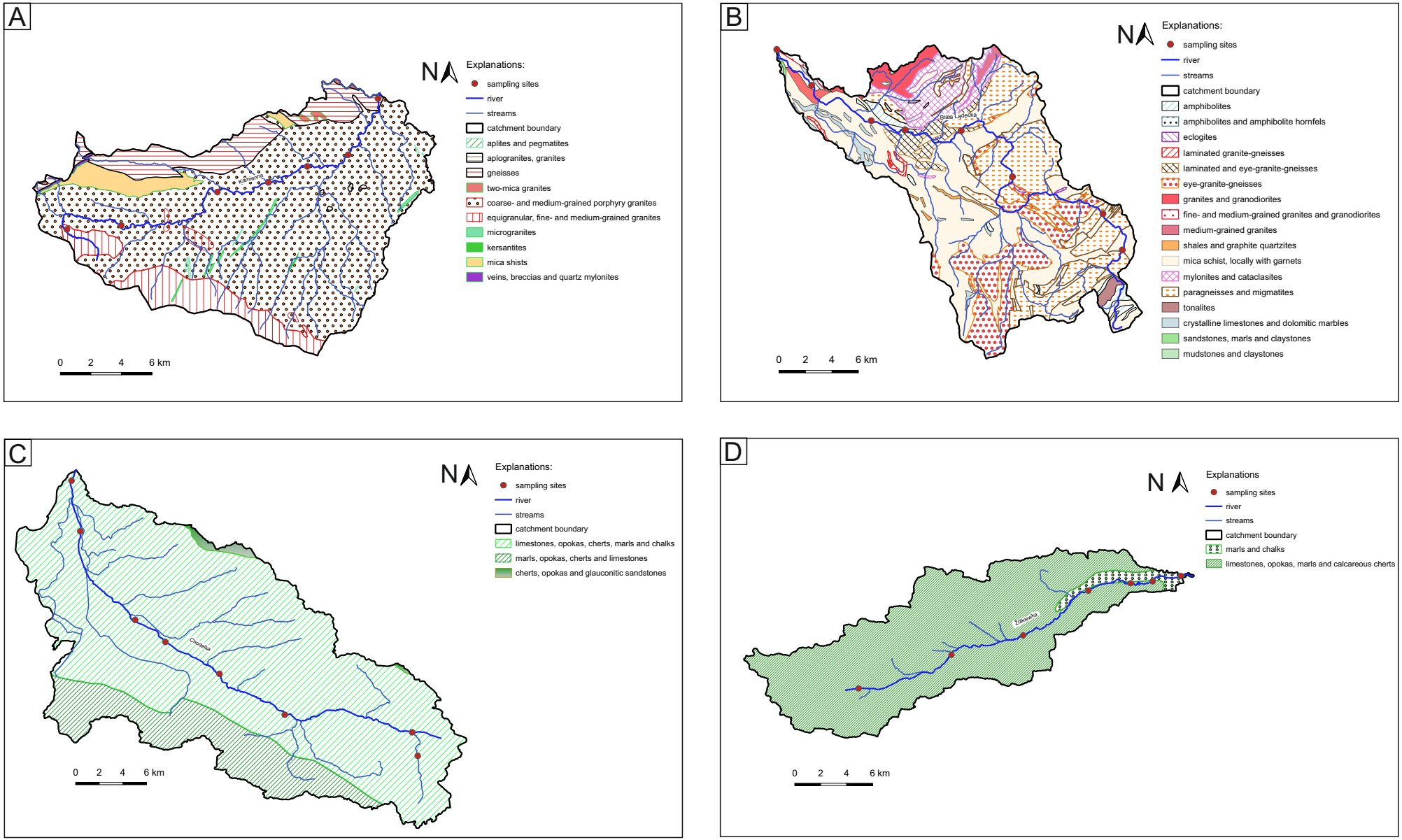

APPENDIX 2

Geological covered maps: A – Kamienna catchment area, B – Biała Lądecka catchment area according to Malinowski and Sawicki (1988a) and Milewicz et al. (1989a)

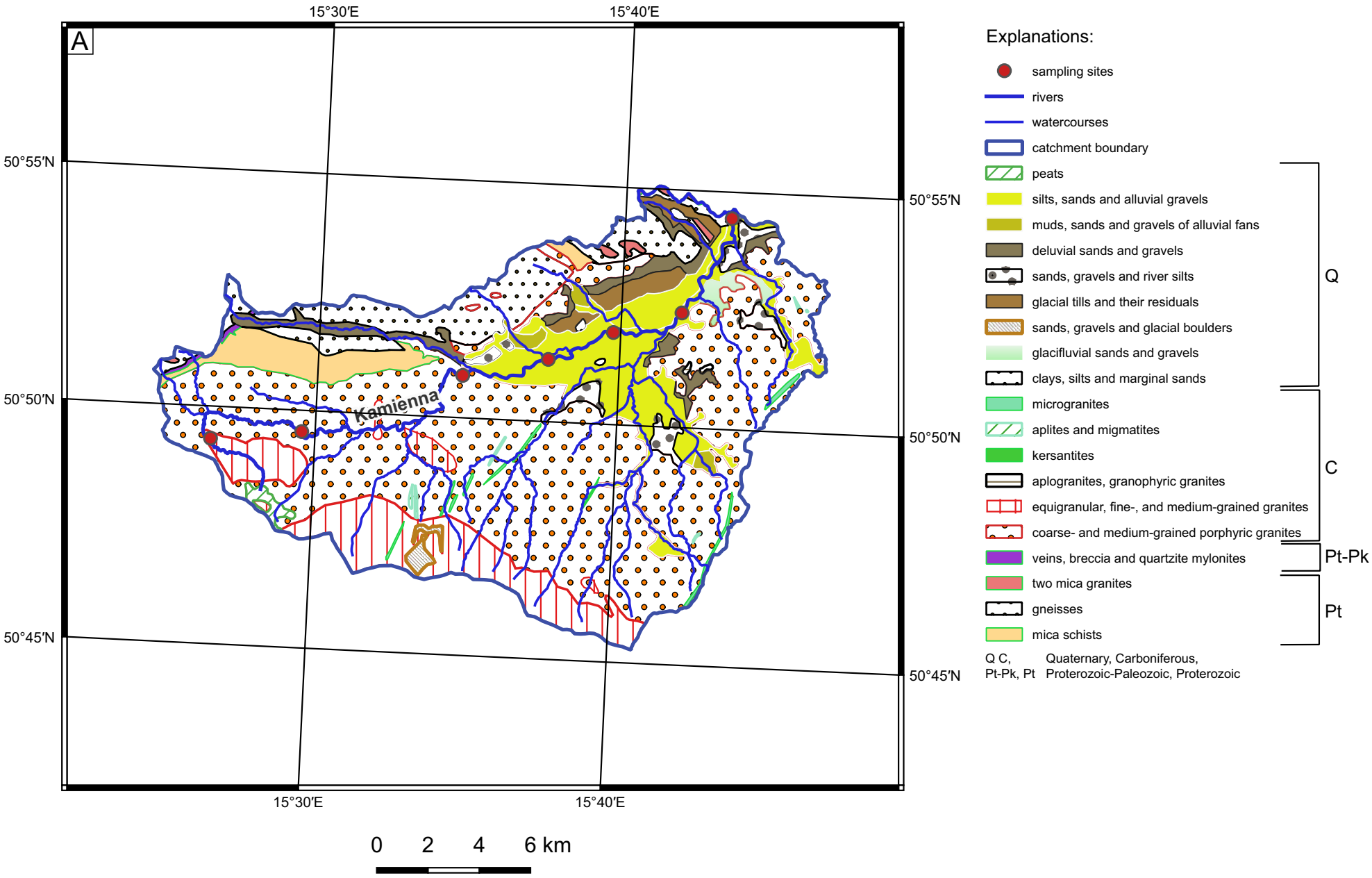

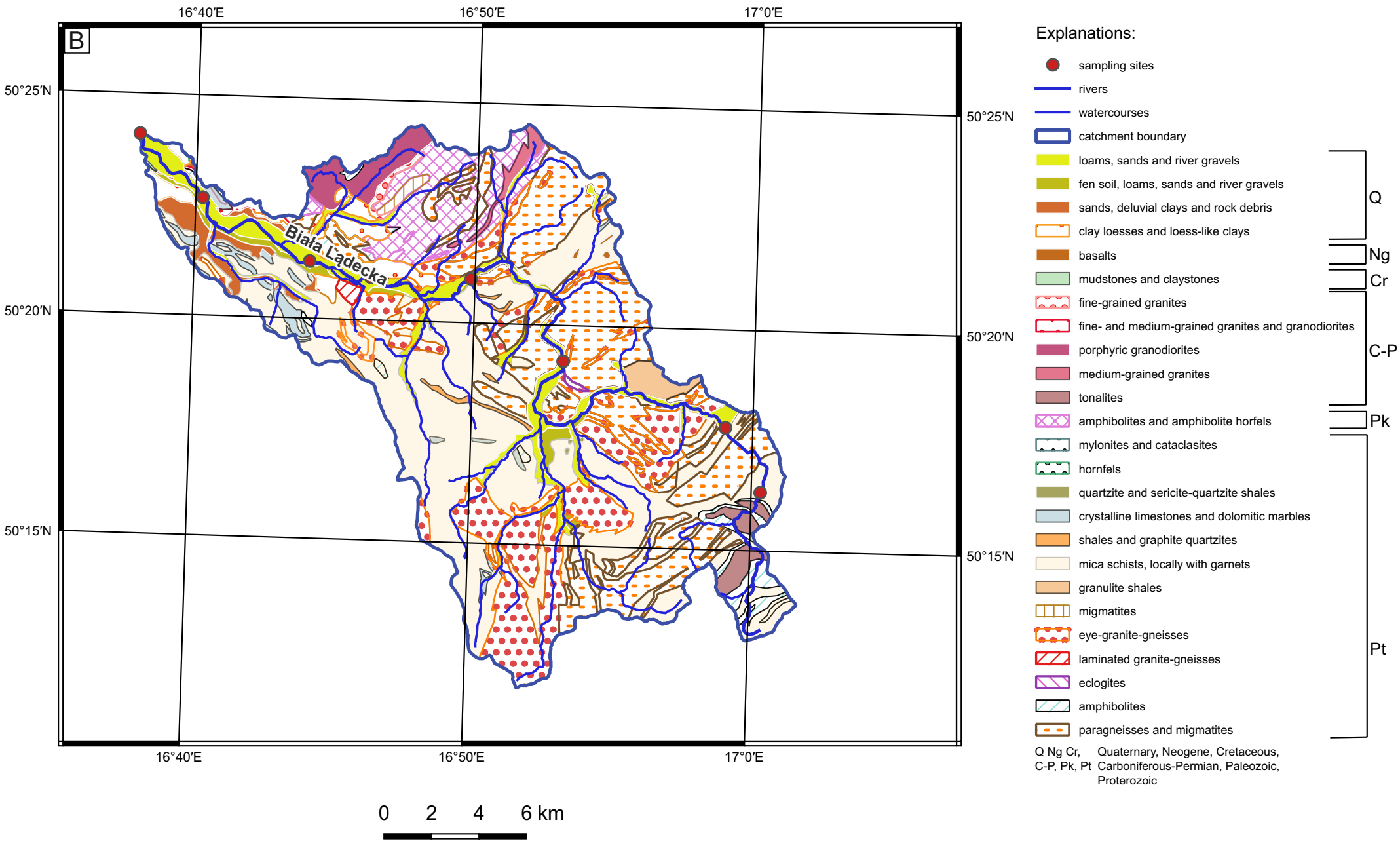

APPENDIX 3

Geomorphological maps of the Kamienna and Biała Lądecka catchment areas and location of sampling sites according to Lisicki (2008); Cymerman et al. (2011); Bobiński (2015); Cymerman and Badura (2019); Cwojdziński (2020) and Morawski (2020)

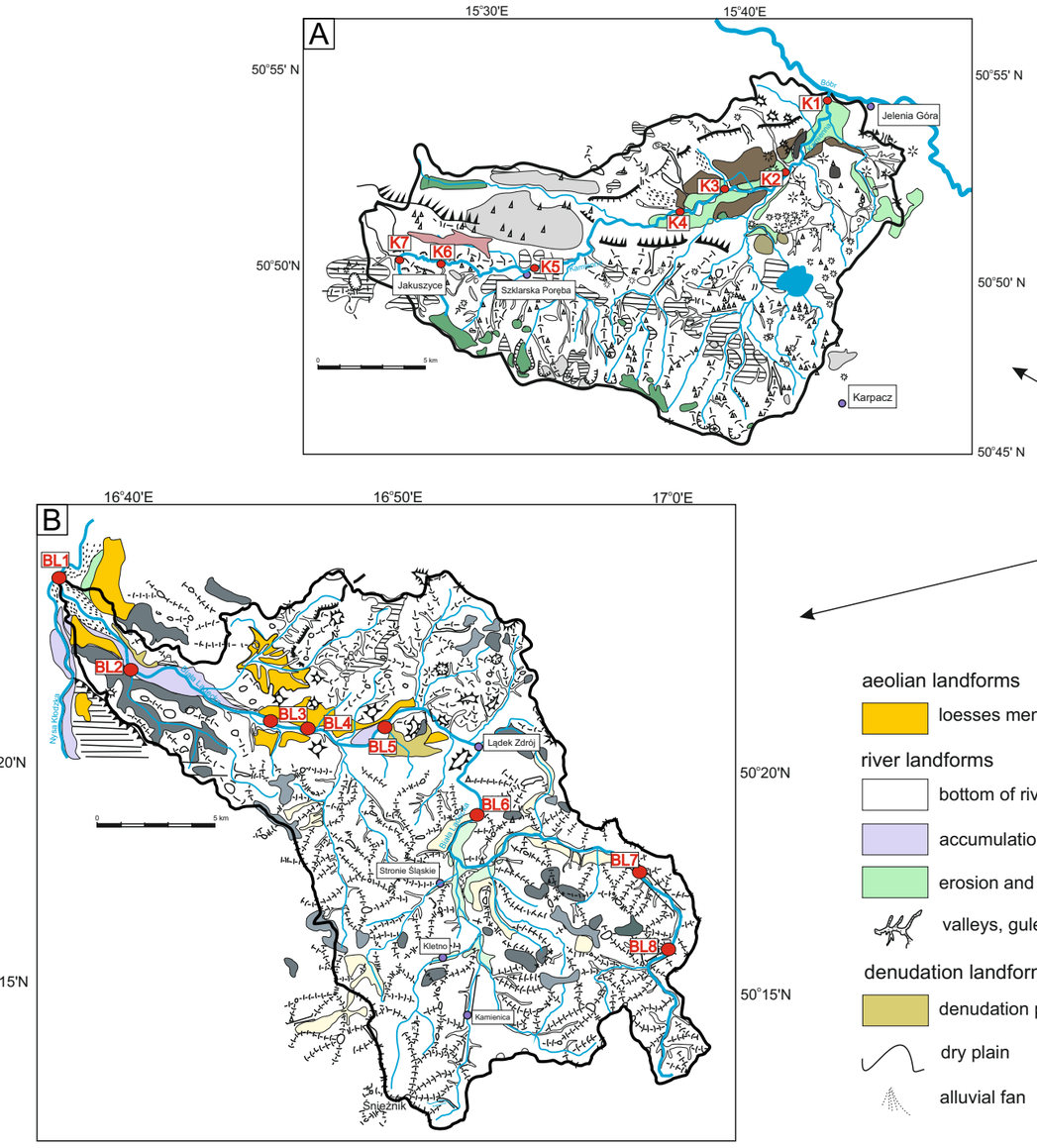

APPENDIX 4

Geological covered maps: A – Chodelka catchment area, B – Żółkiewka catchment area according to Malinowski and Mojski (1881a); Rzechowski (1997) and Romanek (2011a)

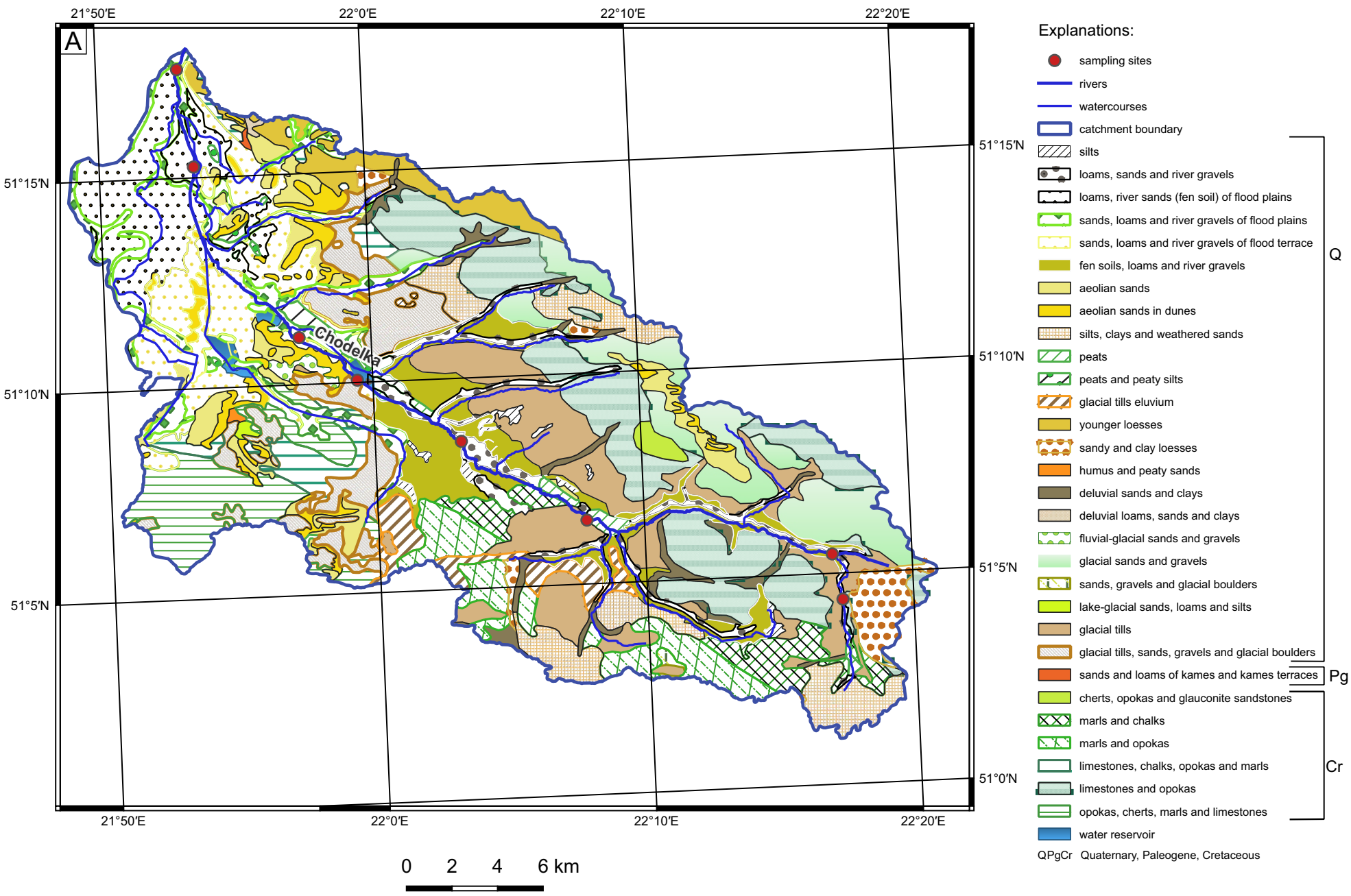

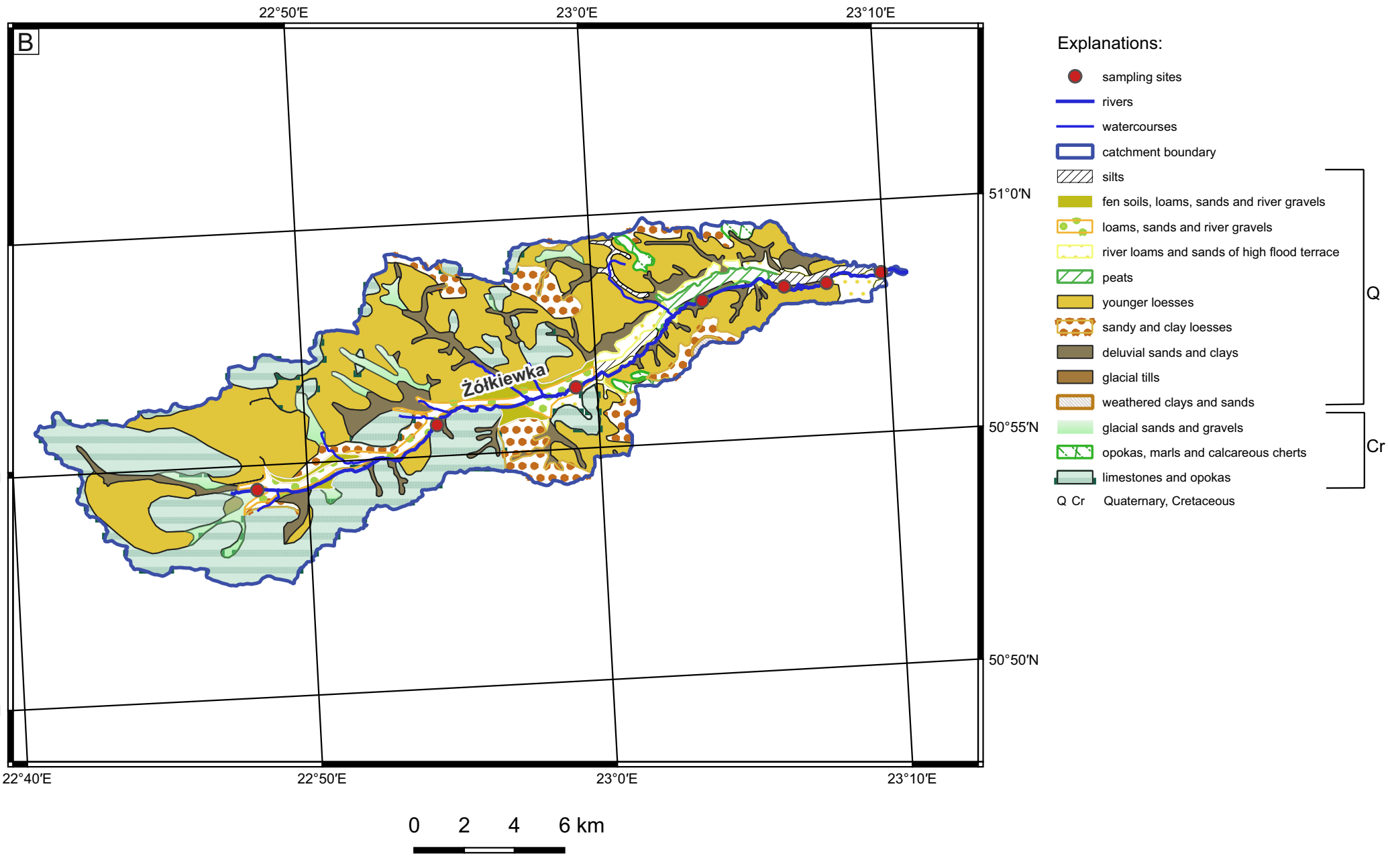

APPENDIX 5

Geomorphological maps of the Chodelka and Żółkiewka catchment areas and location of sampling sites according to Harasimiuk et al. (1988); Albrycht and Brzezina (2000); Marszałek (2001); Kamiński (2023a) and Kamiński (2023b)

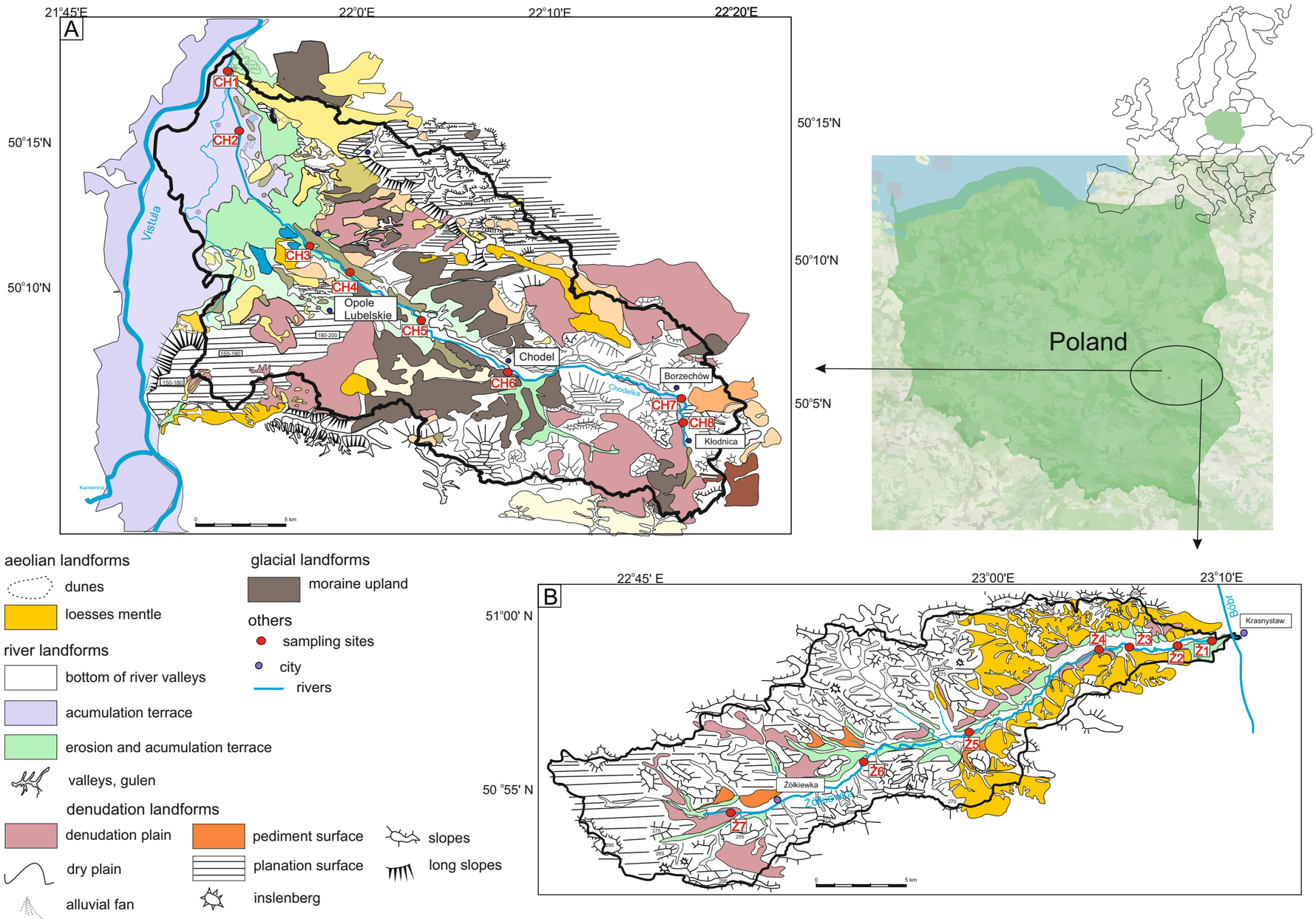

APPENDIX 6

Laboratory number	Sample number	Longitude (DD)	Latitude (DD)	Longitude (DMS)	Latitude (DMS)	Height above sea level (m)	Al_2O_3	MgO	CaO	Na_2O	K_2O	Cu	Rb	Sr	WIP	V	CIA	CIW	PIA	Rb/Sr	Sr/Cu	Bedrock lithology (covered map)	Bedrock lithology (revealed map)
							%	%	%	%	%	ppm	ppm	ppm									
14/22/1	**K1**	15,72546	50,90741	15°43'31.662"E	50°54'26.676"N	324,2	10,52	0,48	0,66	1,98	3,92	13,63	215,06	80,9	54,55	2,60	54,73	70,24	58,48	2,66	5,94	silts, sands and alluvial gravels (holocene)	gneisses (younger Proterozoic)
14/22/2	**K2**	15,70001	50,87360	15°42'00.032"E	50°52'24.947"N	332,9	11,21	0,67	0,89	2,23	3,87	17,86	212,37	96,1	57,54	2,21	54,19	67,95	57,05	2,21	5,38	silts, sands and alluvial gravels (holocene)	coarse- and medium-grained porphyry granites (Upper Carboniferous)
14/22/3	**K3**	15,66251	50,86567	15°39'45.023"E	50°51'56.429"N	341,5	11,07	0,71	0,91	2,04	3,97	19,07	215,08	97,8	56,80	2,26	54,32	68,84	57,48	2,20	5,13	silts, sands and alluvial gravels (holocene)	coarse- and medium-grained porphyry granites (Upper Carboniferous)
14/22/4	**K4**	15,62713	50,85520	15°37'37.685"E	50°51'18.732"N	355,7	10,94	0,50	0,63	1,97	4,01	18,61	211,82	78,5	55,20	2,70	55,63	71,38	60,07	2,70	4,22	silts, sands and alluvial gravels (Holocene)	coarse- and medium-grained porphyry granites (Upper Carboniferous)
14/22/5	**K5**	15,58018	50,84821	15°34'48.665"E	50°50'53.549"N	399,3	10,23	0,41	0,58	1,95	4,15	9,16	224,35	73,6	55,83	2,78	53,89	70,59	57,38	3,05	8,03	coarse- and medium-grained porphyry granites (Upper Carboniferous)	coarse- and medium-grained porphyry granites (Upper Carboniferous)
14/22/6	**K6**	15,49254	50,82590	15°29'33.161"E	50°49'33.227"N	749,6	10,30	0,23	0,25	1,80	4,52	4,05	230,36	47,3	56,25	3,80	55,35	75,10	61,29	4,87	11,68	coarse- and medium-grained porphyry granites (Upper Carboniferous)	coarse- and medium-grained porphyry granites (Upper Carboniferous)
14/22/7	**K7**	15,44226	50,82205	15°26'32.140"E	50°49'19.370"N	854,0	11,73	0,42	0,31	1,94	4,79	6,66	257,13	63,3	60,52	3,51	56,75	75,75	63,54	4,06	9,50	fine- and medium-grained granites (Upper Carboniferous)	equigranular, fine- and medium-grained granites (Upper Carboniferous)
14/22/8	**BL1**	16,63261	50,40140	16°37'57.390"E	50°24'05.022"N	296,6	11,60	0,86	1,08	1,92	3,20	13,24	137,87	131,4	50,00	2,06	57,47	69,37	61,37	1,05	9,92	silts, sands and alluvial gravels (Holocene)	fine- and medium-grained granites and granodiorites (Carboniferous)
14/22/9	**BL2**	16,67081	50,37785	16°40'14.915"E	50°22'40.265"N	315,9	10,73	1,04	1,46	1,74	2,81	31,65	128,38	130,1	46,49	1,69	55,63	66,04	58,22	0,99	4,11	silts, sands and alluvial gravels (Holocene)	mica schists, locally with garnets (younger Proterozoic)
14/22/10	**BL3**	16,73519	50,35497	16°44'06.683"E	50°21'17.885"N	346,0	10,51	0,85	1,00	1,78	3,06	15,47	138,73	105,4	47,29	2,00	56,60	68,89	60,26	1,32	6,81	silts, sands and alluvial gravels (Holocene)	mica schists, locally with garnets (younger Proterozoic)
14/22/11	**BL4**	16,77151	50,34952	16°46'17.423"E	50°20.58.271"N	363,1	10,74	0,83	0,88	1,69	3,07	16,72	136,82	102,9	46,18	2,17	58,23	71,03	62,87	1,33	6,15	silts, sands and alluvial gravels (Holocene)	mica schists, locally with garnets (younger Proterozoic)
14/22/12	**BL5**	16,83099	50,35002	16°49'51.575"E	50°21'00.077"N	394,6	10,72	0,73	0,99	1,93	3,31	14,71	147,61	121,1	50,44	2,10	55,61	68,30	58,93	1,22	8,23	silts, sands and alluvial gravels (Holocene)	laminated and mesh granite-gneisses (older Proterozoic)
14/22/13	**BL6**	16,88684	50,31977	16°53'12.618"E	50°19'11.165"N	457,4	10,92	0,70	0,86	1,90	3,31	14,51	157,39	116,9	49,75	2,24	56,90	69,96	61,01	1,35	8,06	silts, sands and alluvial gravels (Holocene)	paragneisses and migmatites (younger Proterozoic)
14/22/14	**BL7**	16,98387	50,29632	16°59'01.932"E	50°17'46.745"N	623,1	11,64	2,79	3,24	2,19	2,39	17,14	109,04	177,7	56,43	0,86	49,07	55,08	48,81	0,61	10,37	silts, sands and alluvial gravels (Holocene)	mica schists, locally with garnets (younger Proterozoic) and paragneisses and migmatites (younger Proterozoic)
14/22/15	**BL8**	17,00548	50,27208	17°00'19.739"E	50°16'19.499"N	692,4	13,47	1,78	2,17	2,16	2,59	18,78	101,58	239,7	52,35	1,36	56,66	64,24	58,72	0,42	12,76	mica schists, locally with garnets (younger Proterozoic)	mica schists, locally with garnets (younger Proterozoic)
14/22/16	**CH1**	21,88447	51,29301	21°53'04.109"E	51°17'34.823"N	120,6	1,39	0,04	1,19	0,23	0,52	2,25	17,40	52,8	9,68	0,74	30,92	35,35	24,55	0,33	23,47	silts, sands (muds) of flood plains (Holocene)	limestones, chalks, opokas and marls (Upper Cretaceous)
14/22/17	**CH2**	21,89269	51,25430	21°53'33.684"E	51°15'15.473"N	123,5	1,40	0,03	0,82	0,22	0,51	2,32	17,17	30,5	8,53	1,01	36,79	43,04	31,40	0,56	13,15	silts, sands (muds) of flood plains (Holocene)	limestones, chalks, opokas and marls (Upper Cretaceous)
14/22/18	**CH3**	21,95479	51,18529	21°57'17.261"E	51°11'07.037"N	138,6	1,08	0,01	0,68	0,16	0,44	2,22	14,81	32,5	6,97	1,02	35,34	41,87	28,70	0,46	14,64	sands, silts and alluvial gravels of flood terrace (Upper Pleistocene)	limestones, chalks, opokas and marls (Upper Cretaceous)
14/22/19	**CH4**	21,99030	51,16757	21°59'25.092"E	51°10'03.239"N	140,6	1,58	0,68	2,57	0,21	0,50	181,97	18,44	49,9	14,60	0,31	22,13	23,95	17,15	0,37	0,27	sands, silts and alluvial gravels of flood terrace (Upper Pleistocene)	limestones, chalks, opokas and marls (Upper Cretaceous)
14/22/20	**CH5**	22,05397	51,14172	22°03'14.286"E	51°08'30.198"N	152,4	4,00	0,25	7,91	0,50	1,07	10,64	38,51	230,9	34,54	0,33	19,64	20,83	15,75	0,17	21,70	silts, sands and alluvial gravels (Holocene)	marls and chalks (Upper Cretaceous)
14/22/21	**CH6**	22,13066	51,10855	22°07'50.381"E	51°06'30.768"N	164,3	3,04	0,12	4,22	0,49	0,97	6,21	31,18	128,5	23,84	0,47	24,19	26,39	19,01	0,24	20,69	glacial tills (Neopleistocene)	marls and chalks (Upper Cretaceous)
14/22/22	**CH7**	22,28342	51,09097	22°17'00.300"E	51°05'27.504"N	196,8	1,23	0,42	0,95	0,17	0,49	1,83	15,72	24,5	9,31	0,57	32,65	38,00	25,85	0,64	13,39	silts, sands (muds) and alluvial gravels (Holocene)	limestones and opokas (Upper Cretaceous)
14/22/23	**CH8**	22,28886	51,07295	22°17'19.902"E	51°04'22.608"N	204,2	4,66	0,23	0,71	0,49	1,38	6,69	48,93	67,5	18,68	2,30	56,48	68,97	60,16	0,72	10,09	silts, sands and alluvial gravels (Holocene)	limestones and opokas (Upper Cretaceous)
14/22/24	**Ž1**	23,16459	50,97384	23°09'52.535"E	50°58'25.824"N	180,0	1,07	0,09	0,43	0,15	0,40	3,51	13,20	23,9	6,12	1,20	42,27	50,99	38,25	0,55	6,81	silts and alluvial sands of high food terrace (Upper Pleistocene)	marls and chalks (Upper Cretaceous)
14/22/25	**Ž2**	23,13333	50,97113	23°08'00.000"E	50°58'16.056"N	185,4	1,32	0,04	1,00	0,20	0,50	2,37	16,36	46,6	8,75	0,83	32,93	38,07	26,62	0,35	19,66	deluvial sands and clays (Holocene)	opokas, marls and marly opokas (Upper Cretaceous)
14/22/26	**Ž3**	23,10912	50,97069	23°06'32.825"E	50°58'14.466"N	185,4	4,56	0,45	3,60	0,59	1,26	7,53	44,76	167,8	26,55	0,68	33,93	37,76	29,84	0,27	22,28	deluvial sands and clays (Holocene)	opokas, marls and marly opokas (Upper Cretaceous)
14/22/27	**Ž4**	23,06234	50,96718	23°03'44.424"E	50°58'01.865"N	189,3	2,24	0,12	1,58	0,28	0,72	3,98	24,61	87,5	13,05	0,83	35,26	40,19	30,47	0,28	21,98	deluvial sands and clays (Holocene)	opokas, marls and marly opokas (Upper Cretaceous)
14/22/28	**Ž5**	22,98807	50,93866	22°59'17.057"E	50°56'19.169"N	199,9	6,21	0,48	3,51	0,62	1,70	12,23	63,42	220,4	30,42	0,93	40,19	45,62	37,12	0,29	18,02	silts, sands and alluvial gravels (Holocene)	limestones and opokas (Upper Cretaceous)
14/22/29	**Ž6**	22,90826	50,92783	22°54'29.748"E	50°55'40.193"N	208,6	1,27	0,03	1,02	0,19	0,47	2,19	14,59	46,3	8,42	0,79	32,19	36,95	26,00	0,32	21,14	imestones and opokas (Upper Cretaceous)	limestones and opokas (Upper Cretaceous)
14/22/30	**Ž7**	22,80457	50,90790	22°48'16.458"E	50°54'28.446"N	226,9	2,64	0,38	2,90	0,31	0,80	5,96	28,32	88,9	18,09	0,52	28,42	31,34	23,48	0,32	14,92	glacifluvial sands and gravels (Mesopleistocene)	limestones and opokas (Upper Cretaceous)

Explanations: Samples analized on SEM